



HAL
open science

Modulation of the gut microbiota impacts non-alcoholic fatty liver disease: a potential role for bile acids

Aafke Wf Janssen, Tom Houben, Saeed L Katiraei, Wieneke Dijk, Lily L Boutens, Nieke van Der Bolt, Zeneng L Wang, Mark J Brown, Stanley L Hazen, Stéphane L Mandard, et al.

► **To cite this version:**

Aafke Wf Janssen, Tom Houben, Saeed L Katiraei, Wieneke Dijk, Lily L Boutens, et al.. Modulation of the gut microbiota impacts non-alcoholic fatty liver disease: a potential role for bile acids. *Journal of Lipid Research*, 2017, 58 (7), pp.1399-1416. 10.1194/jlr.M075713 . inserm-01527524

HAL Id: inserm-01527524

<https://inserm.hal.science/inserm-01527524>

Submitted on 24 May 2017

HAL is a multi-disciplinary open access archive for the deposit and dissemination of scientific research documents, whether they are published or not. The documents may come from teaching and research institutions in France or abroad, or from public or private research centers.

L'archive ouverte pluridisciplinaire **HAL**, est destinée au dépôt et à la diffusion de documents scientifiques de niveau recherche, publiés ou non, émanant des établissements d'enseignement et de recherche français ou étrangers, des laboratoires publics ou privés.

Modulation of the gut microbiota impacts non-alcoholic fatty liver disease: a potential role for bile acids

Aafke WF Janssen¹, Tom Houben², Saeed Katiraei³, Wieneke Dijk¹, Lily Boutens^{1,4}, Nieke van der Bolt¹, Zeneng Wang⁵, J Mark Brown⁵, Stanley L Hazen⁵, Ronit Shiri-Sverdlov², Folkert Kuipers⁶, Ko Willems van Dijk^{3,7}, Jacques Vervoort⁸, Rinke Stienstra^{1,4}, Guido JEJ Hooiveld¹, Sander Kersten¹

¹Nutrition, Metabolism and Genomics Group, Wageningen University, 6708 WE Wageningen, The Netherlands

²Department of Molecular Genetics, Maastricht University, 6200 MD Maastricht, The Netherlands

³Department of Human Genetics, Leiden University Medical Center, 2300 RC Leiden, The Netherlands

⁴Department of Medicine, Radboud University Medical Center, 6525 GA Nijmegen, The Netherlands

⁵Department of Cellular and Molecular Medicine, Cleveland Clinic Lerner Research Institute, Cleveland, Ohio 44195, USA

⁶Department of Pediatrics, University Medical Center Groningen, 9713 GZ Groningen, The Netherlands

⁷Department of Medicine, Leiden University Medical Center, 2300 RC Leiden, The Netherlands

⁸Laboratory of Biochemistry, Wageningen University, 6708 WE Wageningen, The Netherlands

Running title: Gut microbiota affects NAFLD development

Abbreviations: α SMA, alpha smooth muscle actin; GG, guar gum; HFCFD, high fat/high cholesterol/high fructose diet; IL, interleukin; LPS, lipopolysaccharide; MCP-1, monocyte chemoattractant protein-1; NAFLD, non-alcoholic fatty liver disease; NASH, non-alcoholic steatohepatitis; RS, resistant starch; SCFA, short chain fatty acid; TCA, taurocholic acid; TIMP, tissue inhibitor of metalloproteinases; TMA, trimethylamine; TMAO, trimethylamine N-oxide; TNF α , tumor necrosis factor alpha.

Correspondance should be addressed to author: Sander Kersten, PhD, Nutrition, Metabolism and Genomics group, Division of Human Nutrition, Wageningen University, Stippeneng 4, 6708 WE Wageningen, The Netherlands. Phone: +31 317 485787; Email: sander.kersten@wur.nl.

Disclosures: The authors have nothing to disclose.

Transcript Profiling: Array data have been submitted to the Gene Expression Omnibus under accession number GSE76087 (<https://www.ncbi.nlm.nih.gov/geo/query/acc.cgi?token=epqticwcnlalyx&acc=GSE76087>).

Abstract

Non-alcoholic fatty liver disease (NAFLD) is rapidly becoming the most common liver disease worldwide, yet the pathogenesis of NAFLD is only partially understood. Here, we investigated the role of the gut bacteria in NAFLD by stimulating the gut bacteria via feeding mice the fermentable dietary fiber guar gum and suppressing the gut bacteria via chronic oral administration of antibiotics.

Guar gum feeding profoundly altered the gut microbiota composition, in parallel with reduced diet-induced obesity and improved glucose tolerance. Strikingly, despite reducing adipose tissue mass and inflammation, guar gum enhanced hepatic inflammation and fibrosis, concurrent with markedly elevated plasma and hepatic bile acid levels. Consistent with a role of elevated bile acids in the liver phenotype, treatment of mice with taurocholic acid stimulated hepatic inflammation and fibrosis. In contrast to guar gum, chronic oral administration of antibiotics effectively suppressed the gut bacteria, decreased portal secondary bile acid levels, and attenuated hepatic inflammation and fibrosis. Neither guar gum or antibiotics influenced plasma lipopolysaccharide levels.

In conclusion, our data indicate a causal link between changes in gut microbiota and hepatic inflammation and fibrosis in a mouse model of NAFLD, possibly via alterations in bile acids.

Keywords: gut microbiota, antibiotics, hepatic fibrosis, hepatic inflammation, liver, bile acids and salts, obesity, inflammation, intestine

Introduction

The worldwide epidemic of obesity is the primary driver for the global increase in the prevalence of type 2 diabetes and non-alcoholic fatty liver disease (NAFLD)(1). While caloric overconsumption and the associated positive energy balance are the sine qua non of obesity development, emerging evidence implicates gut microbes in the promotion of obesity and related metabolic disturbances (2–5).

The human intestine contains a variety of microbiota, mainly consisting of bacteria and complemented by other microorganisms such as fungi, protozoa and viruses. The gut microbiota form a mutualistic relationship with the host and have an important role in host health. Besides protecting the host against invading pathogenic microorganisms, intestinal bacteria facilitate the digestion of otherwise indigestible carbohydrates, produce essential vitamins, stimulate the development of the immune system and maintain tissue homeostasis (6, 7). In recent years, the gut microbiota have increasingly been connected with a number of diseases, including irritable bowel syndrome, Crohn's disease, obesity, type 2 diabetes, atherosclerosis and NAFLD (5, 8–10).

NAFLD describes a spectrum of related liver diseases ranging from simple steatosis to non-alcoholic steatohepatitis (NASH), liver fibrosis, and cirrhosis(11). Although the exact pathogenesis of NAFLD is unknown, multiple factors likely contribute to the progression of NAFLD, including genetic predisposition, lipid overload, and inflammatory insults. Indeed, it is believed that inflammatory mediators released locally or derived from tissues such as the intestine and adipose tissue play an important role in the progression of steatosis to NASH (12, 13).

Recent studies have raised the possibility that NAFLD may be related to disturbances in the gut microbial composition. In particular, it was found that the gut microbial composition was different between healthy individuals and patients with NAFLD (14, 15). Furthermore, mouse

studies suggest that changes in the gut microbial community may impact the development of hepatic steatosis (16), inflammation (17, 18) and fibrosis (18).

To further elaborate the concept that the gut microbiota may affect the development of NAFLD, we studied the influence of modulation of the gut microbiota on NAFLD. To that end, in a mouse model of NAFLD, we stimulated the gut bacteria by feeding mice the highly fermentable dietary fiber guar gum, using the poorly fermentable dietary fiber resistant starch as control. Inasmuch as guar gum escapes digestion in the small intestine and is thought to act exclusively via bacterial fermentation and concomitant alterations in gut microbiota, feeding guar gum is an attractive strategy to study the role of the gut microbes in NAFLD. Additionally, in the same mouse model of NAFLD, we studied the effect on NAFLD of suppressing the gut bacteria using a mixture of antibiotics.

Overall, our data indicate that the gut microbiota have a marked impact on NAFLD. Specifically, specific modulation of the gut microbiota by feeding guar gum worsened features of NAFLD, whereas suppression of the gut bacteria using oral antibiotics protected against NAFLD, possibly via changes in the portal delivery of bile acids.

Methods

Animals and diet

Animal studies were performed using pure-bred male C57Bl/6 mice. Mice were individually housed in temperature- and humidity-controlled specific pathogen-free conditions. Mice had *ad libitum* access to food and water. In study 1, 11-week-old mice received a low fat diet or a high fat/high cholesterol/high fructose diet (HFCFD) for 18 weeks, providing 10% or 45% energy as triglycerides (formula D12450B or D12451 from Research Diets, Inc., manufactured by Research Diet Services, Wijk bij Duurstede, Netherlands). The fat source of this HFCFD was replaced by safflower oil and supplemented with 1% cholesterol (Dishman, Veenendaal, Netherlands). Mice receiving the HFCFD were provided with 20% fructose water (wt/vol) to promote development of NAFLD(19). The fiber-enriched diets were identical to the HFCFD (CTRL) except that corn starch and part of the maltodextrin 10 were replaced by 10% (wt/wt) resistant starch (RS) or guar gum (GG). The composition of the diets is shown in Supplemental Table 1. Resistant starch, a retrograded tapioca starch classified as RS type 3 (brand name C* Actistar 11700) and guar gum (brand name Viscogum) were obtained from Cargill R&D Centre Europe (Vilvoorde, Belgium). Bodyweight and food intake were assessed weekly. One mouse fed the GG-enriched diet died during the study for reasons unrelated to the intervention.

In study 2, 10-week-old mice received a high fat/high cholesterol/high fructose diet (CTRL) for 18 weeks, providing 45% energy as triglycerides (formula 58V8 manufactured by TestDiet, St. Louis, USA). This diet was supplemented with 1% cholesterol (Dishman, Veenendaal, Netherlands). The mice received 20% fructose (wt/vol) in the drinking water. The TMAO-enriched diet was identical to the CTRL diet except that 0.296 % of sucrose (wt/wt) was replaced by 0.296% TMAO-dihydrate (wt/wt) (Sigma, Zwijndrecht, The Netherlands) to obtain a final concentration of 0.2% TMAO (wt/wt). Bodyweight and food

intake were assessed weekly. One mouse fed the TMAO-enriched diet died during the study for reasons unrelated to the intervention. One mouse in the CTRL group and one mouse fed the TMAO-enriched diet failed to thrive and were excluded from further analysis.

In study 3, 4 month-old male mice received either chow (CTRL) or chow supplemented with 0.5% (wt/wt) taurocholic acid (TCA) (Calbiochem) for 7 days (20). Bodyweight and food intake were assessed daily.

In study 4, 10-week old mice received a high fat/high cholesterol/high fructose diet (CTRL) for 18 weeks, providing 45% energy as triglycerides (formula 58V8 manufactured by TestDiet, St. Louis, USA). The diet was supplemented with 1% cholesterol (Dishman, Veenendaal, Netherlands). The mice received 20% fructose (wt/vol) in the drinking water. Mice that were given antibiotics received the same CTRL diet with the addition of 1g/l Ampicillin, 1g/l Neomycin sulphate, 1g/l Metronidazole and 0.5g/l Vancomycin in the drinking water for 22 weeks. This antibiotic cocktail has previously been shown to deplete all detectable commensal bacteria (21). Bodyweight and food intake were assessed weekly. One mouse in the CTRL group and one mouse in the antibiotics group failed to thrive and were excluded from further analysis.

At the end of each study, mice were anesthetized using isoflurane and blood was collected by orbital puncture. Mice were euthanized via cervical dislocation after which tissues were excised and weighed and intestinal content was sampled. The mice were not fasted prior to euthanasia (e.g. ad libitum fed state). The animal experiments were approved by the local animal ethics committee of Wageningen University.

Intraperitoneal glucose tolerance test

In study 1, mice were fasted for 5 hours prior to the intraperitoneal glucose tolerance test. During this period fructose water was replaced by tap water. Blood samples were collected

from the tail vein immediately before (t=0 min) and at selected time points after intraperitoneal injection with glucose (0.8 g/kg bodyweight). Glucose was measured using Accu-chek Compact. Plasma concentrations of insulin were quantified after 5 hour fasting according to manufacturer's instructions (Crystal Chem, Downers Grove, USA).

RNA isolation and qPCR

Total RNA was extracted from epididymal white adipose tissue, liver and scrapings of the distal small intestine using TRIzol reagent (Life technologies, Bleiswijk, Netherlands). Subsequently, 500ng RNA was used to synthesize cDNA using iScript cDNA synthesis kit (Bio-Rad Laboratories, Veenendaal, Netherlands). Changes in gene expression were determined by real-time PCR on a CFX384 Real-Time PCR detection system (Bio-Rad Laboratories, Veenendaal, Netherlands) by using SensiMix (Bioline, GC biotech, Alphen aan den Rijn, Netherlands). The housekeeping gene 36b4 or β -actin was used for normalization. Sequences of the used primers are listed in Supplemental Table 2.

Histology/Immunohistochemistry

Hematoxylin and Eosin (H&E) staining of sections was performed using standard protocols. Paraffin-embedded liver sections (5 μ m) were stained for collagen using fast green FCF/Sirius Red F3B. Staining of neutral lipids was performed on frozen liver sections using Oil Red O according to standard protocols.

Visualization of hepatic stellate cells was performed on paraffin-embedded liver sections with an antibody against alpha smooth muscle actin (α SMA)(M0851, Dako, Heverlee, Belgium). To detect macrophages, 5 μ m frozen liver sections were stained for Cd68 Kupffer cells (Cd68 marker, FA11) as described previously (22).

Plasma/serum measurements

In study 1 and 3, blood was collected in EDTA-coated tubes and centrifuged for 15 minutes at 3000 rpm to obtain plasma. In study 2 and 4, blood was collected, allowed to clot for 45 minutes and centrifuged for 15 minutes at 3000 rpm to obtain serum. The mice were not fasted prior to blood collection. Plasma and serum alanine aminotransferase activity was measured with a kit from Abcam (Cambridge, UK). The commercially available Limulus Amebocyte Lysate assay (Lonza, Walkerville, USA) was used to quantify plasma and portal serum endotoxin levels. Plasma concentration of total bile acids were determined using a colorimetric assay kit (Diazyme Laboratories, Poway, USA). Free and conjugated bile acid subspecies were quantified by liquid chromatography tandem MS (LC-MS/MS) using a SHIMADZU liquid chromatography system (SHIMADZU, Kyoto, Japan) and tandem AB SCIEX API-3200 triple quadrupole mass spectrometry (AB SCIEX, Framingham, USA) as previously described (23). TMA and TMAO plasma levels and TMAO serum levels were quantified by stable isotope dilution liquid chromatography tandem mass spectrometry as previously described (24, 25).

Fecal measurements

In study 1, during the 6th week of dietary intervention feces were collected over a period of 48 hours. Total lipids and free fatty acids were measured in the fecal samples as mentioned by Govers *et al* .(26). Briefly, 100mg of fecal samples were weighed, dried and acidified using HCl. Lipids were then extracted using petroleum and diethyl ether. Ether fraction was collected, evaporated and the total lipids were weighed.

Free and conjugated bile acid subspecies in the feces, collected at the end of the dietary intervention in study 1 and 4, were determined by capillary gas chromatography (Agilent 6890, Amstelveen, the Netherlands) as described previously (27).

Microarray analysis

Microarray analysis was performed on liver samples from 8 mice of the CTRL group and 8 mice of the GG group. RNA was isolated as described above and subsequently purified using the RNeasy Microkit from Qiagen (Venlo, The Netherlands). RNA integrity was verified with RNA 6000 Nanochips on a Agilent 2100 bioanalyzer (Agilent Technologies, Amsterdam, the Netherlands). Purified RNA (100 ng) was labeled with the Ambion WT expression kit (Invitrogen, Carlsbad, USA) and hybridized to an Affymetrix Mouse Gene 1.1 ST array plate (Affymetrix, Santa Clara, USA). Hybridization, washing, and scanning were carried out on an Affymetrix GeneTitan platform according to the instruction by the manufacturer. Arrays were normalized using the Robust Multiarray Average method (28, 29). Probe sets were defined according to Dai *et al.* (30). In this method, probes are assigned to Entrez IDs as a unique gene identifier. The p-values were calculated using an Intensity-Based Moderated T-statistic (IBMT) (31). The q-value was calculated as a measure of significance for false discovery rate (32). To identify the pathways most significantly altered in the livers of the GG group compared to the CTRL group, Ingenuity Pathway Analysis (Ingenuity Systems, Redwood City, USA) was performed. Input criteria were a relative fold change equal to or above 1.3 and a q-value equal to or below 0.01. Array data have been submitted to the Gene Expression Omnibus under accession number GSE76087.

A publicly available dataset (GSE34730) was downloaded from Gene Expression Omnibus and further processed as described above to obtain individual gene expression data. Ingenuity Pathway Analysis was performed on genes induced by deoxycholic acid by at least two-fold.

Western blot

Liver homogenates were prepared by lysing liver tissue in ice-cold Pierce IP lysis buffer (ThermoScientific, Rockford, USA) containing complete protease inhibitor and PhosSTOP phosphatase inhibitor (both from Roche, Mannheim, Germany). Equal amounts of protein were loaded on a Mini Protean TGX gel, 4-15% and subsequently transferred to a PVDF membrane (both from Bio-Rad Laboratories, Veenendaal, The Netherlands). The primary antibodies for TIMP1 (Abcam, Cambridge, UK) and HSP90 (Cell Signalling) were incubated at 4°C overnight followed by incubation with the appropriate secondary peroxidase-conjugated antibody (Sigma, Zwijndrecht, The Netherlands). Protein bands were visualized using an Enhanced Chemiluminescent substrate (Bio-Rad Laboratories, Veenendaal, The Netherlands).

Liver measurements

For liver triglyceride measurement, livers were homogenized in a buffer containing 10mM Tris, 2mM EDTA and 250mM sucrose at pH 7.5 in a Tissue Lyser II (Qiagen, Hilden, Germany) to obtain 2% homogenates. Triglycerides were subsequently quantified using a Triglycerides liquicolor^{mono} from HUMAN Diagnostics (Wiesbaden, Germany). 4-hydroxyproline content was determined spectrophotometrically in liver hydrolysates as described previously (33).

For hepatic myeloperoxidase activity, liver homogenates were prepared and myeloperoxidase activity was measured according to manufacturer's instructions (Abcam, Cambridge, UK).

For the quantification of liver total bile acid content, livers were homogenized in 75% ethanol, incubated at 50°C and centrifuged. After the collection of the supernatant, the

concentration of total bile acids were determined using a colorimetric assay kit (Diazyme Laboratories, Poway, USA).

FACS analysis

Epididymal white adipose tissue was isolated, minced and digested with 1.5 mg/ml collagenase type 2 (Sigma, Zwijndrecht, The Netherlands) in DMEM containing 0.5% fatty acid free BSA for 45 minutes at 37°C by shaking. Cell suspensions were filtered through a 100µM filter and centrifuged at 200g for 10 minutes. Floating mature adipocytes were discarded and the stromal vascular cell pellet was resuspended in erythrocyte lysis buffer for 5 minutes. Cells were washed twice with FACS buffer (PBS + 1% BSA) and incubated with fluorescently labeled antibodies including CD45-ECD (Beckman Coulter, Fullerton, USA) , F4/80-FITC and Cd11b-PE (Biolegend, San Diego, USA). Samples were analyzed using a FC500 Flow Cytometer (Beckman Coulter, Fullerton, USA).

DNA extraction

In study 1, fecal samples derived from the second part of the colon were suspended in 10 mM Tris, 1mM EDTA, 0.5% SDS and 0.2mg/ml Proteinase K (ThermoScientific, Rockford, USA). After addition of 0.1-0.25mm and 4mm glass beads, buffered phenol (Invitrogen, Carlsbad, USA) was added and cells were lysed by mechanical disruption using a bead beater (MP biomedical, Santa Ana, USA) for 3 minutes. DNA was subsequently extracted using phenol:chloroform:isoamylalcohol [25:24:1] (Invitrogen, Carlsbad, USA), precipitated with isopropanol and washed with 70% ethanol.

In study 4, fecal samples (~15-60mg) derived from the second part of the colon were suspended in 500 uL S.T.A.R. buffer (Roche). After addition of 0.1mm zirconia and 2.5mm glass beads (BioSpec, Bartlesville, USA), cells were lysed by mechanical disruption using a

bead beater (MP biomedical, Santa Ana, USA) for 3x1 minute. DNA was subsequently extracted and purified using Maxwell 16 System (Promega). In brief, homogenates (250 µL) were transferred to a prefilled reagent cartridge (Maxwell® 16 Tissue LEV Total RNA Purification Kit, Custom-made, Promega). Sixteen samples were processed at the same time. After 30 minutes the purification process was completed and DNA was eluted in 50 µL of water (Nuclease free)(Promega).

16s rRNA gene sequencing

For 16s rRNA gene sequencing DNA samples were send to the Broad Institute of MIT and Harvard (Cambridge, USA). Microbial 16s rRNA gene was amplified targeting the hyper-variable region V4 using forward primer 515F (5'-GTGCCAGCMGCCGCGGTAA-3') and the reverse primer 806R (5'- GGACTACHVGGGTWTCTAAT-3'). The cycling conditions consisted of an initial denaturation of 94°C for 3 min, followed by 25 cycles of denaturation at 94°C for 45 sec, annealing at 50 °C for 60 sec, extension at 72°C for 5 min, and a final extension at 72°C for 10 min. Sequencing was performed using the Illumina MiSeq platform generating paired-end reads of 175 bp in length in each direction. Overlapping paired-end reads were subsequently aligned. Detailed of this protocol are as previously described (34).

Raw sequence data quality was assessed using FastQC, version: 0.11.2 (<http://www.bioinformatics.babraham.ac.uk/projects/fastqc/>). Reads quality was checked with Sickle, version: 1.33 (<https://github.com/najoshi/sickle>) and low quality reads were removed. For visualising the taxonomic composition of the fecal microbiota and further beta diversity analysis, QIIME, version: 1.9.0 was used (35). In brief, closed reference OTU picking with 97% sequence similarity against GreenGenes 13.8 reference database was done. Jackknifed beta-diversity of unweighted UniFrac distances with 10 jackknife replicates was measured at rarefaction depth of 22000 reads/sample. For statistical significance, biological relevance and

visualisation we used linear discriminant analysis (LDA) effect size (LEfSe) method (<https://bitbucket.org/biobakery/biobakery/wiki/lefse>)(36).

Bacterial 16s rRNA gene and fungal ITS1-5.8S-ITS2 region quantification

In study 4, real-time PCR was used to quantify 16s rRNA gene and ITS1-5.8S-ITS2 region in equal amounts of extracted DNA on a CFX384 Real-Time PCR detection system (Bio-Rad Laboratories, Veenendaal, Netherlands) by using SensiMix (Bioline, GC biotech, Alphen aan den Rijn, Netherlands). 16s rRNA gene was amplified using the forward primer 1369F (5'-CGGTGAATACGTTCYCGG-3') and the reverse primer 1492R (5'-GGWTACCTTGTTACGACTT-3')(37). The cycling conditions consisted of an initial denaturation of 95°C for 5 min, followed by 40 cycles of denaturation at 95°C for 15 sec, annealing at 60 °C for 30 sec and extension at 72°C for 30 sec. The ITS1-5.8S-ITS2 region was amplified using universal fungal primers V9D (5'-TTAAGTCCCTGCCCTTTGTA-3') and LS266 (5'-GCATTCCCAAACAACACTCGACTC-3') encompassing highly conserved regions encoding fungal rDNA (38). The cycling conditions consisted of an initial denaturation of 94°C for 10 min, followed by 30 cycles of denaturation at 94°C for 30 sec, annealing at 58 °C for 30 sec, extension at 72°C for 30 sec and a final extension at 72°C for 10 min.

¹H NMR spectroscopy

Contents of the cecum and first part of the colon were collected, mixed with phosphate buffer (pH 8) containing 10% deuterium oxide (D₂O) and stored at -20°C. For short chain fatty acid (SCFA), ethanol and choline quantification samples were thawed, mixed and centrifuged at 14000 rpm for 5 minutes. Supernatant was collected and diluted in phosphate buffer containing 2mM maleic acid as standard. Subsequently, 200µl sample was transferred to 3mm

NMR tubes (Bruker Match System) and measured at 300K in an Avance III NMR spectrometer operated at 600.13 MHz as described previously (39).

Statistical analysis

Data are presented as mean \pm SEM. Statistical significant differences were determined with one way analysis of variance followed by Tukey's post hoc multiple comparison test. Comparisons between two groups were made using two-tailed Student's t-test. $P < 0.05$ was considered as statistically significant. SPSS software (Version 21, SPSS Inc., Chicago, USA) was used for statistical analysis.

Results

High fat/high cholesterol/high fructose diet as model for NAFLD

Feeding mice a diet rich in fat, cholesterol and/or fructose are commonly used strategies to induce NAFLD (40–42). To verify the suitability of the high fat/high cholesterol/high fructose diet (HFCFD) as model for NAFLD, we tested the effect of HFCFD on various relevant parameters in comparison with a commonly used low fat diet. Weight gain, adipose tissue weight and liver weight were significantly higher in the mice fed HFCFD as compared to mice fed the low fat diet (Figure 1A-C). Hepatic lipid storage was markedly higher in mice fed HFCFD, as shown by a five-fold increase in liver triglycerides (Figure 1D) and by Oil Red O staining (Figure 1E). H&E confirmed the presence of microvesicular and macrovesicular steatosis, and showed mild infiltration of immune cells (Figure 1F). Hepatic expression of macrophage markers *Cd68*, *F4/80* and *Cd11c* and pro-inflammatory cytokines *Mcp-1* and *Tnfa* were significantly elevated in mice fed HFCFD, as was the expression of fibrosis markers collagen type I alpha 1 and *Timp1* (Figure 1G). Finally, plasma ALT levels were doubled in mice fed HFCFD (Figure 1H). Taken together, these data show that feeding HFCFD represents a suitable model to study NAFLD.

Dietary guar gum alters colonic microbial composition

To evaluate the potential impact of alterations in the gut microbial community on the development of NAFLD, we fed mice the highly fermentable dietary fiber guar gum (GG) on a background of HFCFD for 18 weeks. Mice fed the poorly fermentable dietary fiber resistant starch (RS) and mice that were not fed any dietary fiber (CTRL) served as negative controls. To assess the effect of GG on colonic microbial composition and the relative abundance of specific gut microbiota taxa, 16s rRNA gene sequencing was performed on faecal samples collected at the end of the dietary intervention. Clustering of 16s rRNA gene sequences by

unweighted UniFrac distances per mouse revealed a sharp clustering of microbiome sequence data of the GG mice, indicating that the colonic microbial community was distinct between CTRL and GG mice. In contrast, the microbiota of the RS mice more closely resembled that of the CTRL mice (Figure 2A). Analysis of the microbiota at various taxonomic levels indicated differences in microbial composition depending on fiber type. In comparison with CTRL, both types of dietary fibers significantly reduced the relative abundance of Deferribacteres and Firmicutes, and increased the relative abundance of Bacteroidetes. The abundance of Actinobacteria was particularly increased in the GG mice. With a relative proportion of 8.23% of all phyla, the phylum Verrucomicrobia was overrepresented in the GG mice, whereas it was almost completely absent in CTRL and RS mice (Figure 2B and Supplemental Table 3).

The differences in microbial community between the RS and GG groups became more apparent at lower taxonomic levels. While GG increased the abundance of the genera *Bifidobacterium* and *Prevotella*, RS had relatively small effects on these genera. The decreased abundance of the phylum Firmicutes for both dietary fibers can be mainly explained by a decrease within the genus *Lactobacillus*. GG also markedly suppressed *SMB53* and *Oscillospira* and increased the abundance of the species *Desulfovibrio C21_c20* (Figure 2C-E and Supplemental Table 3). Overall, these data indicate that GG feeding markedly altered the bacterial composition in the colon.

Modulation of the gut microbiota by guar gum is associated with protection against diet-induced obesity and improved glucose tolerance

Whereas RS did not influence bodyweight gain, GG markedly attenuated bodyweight gain as compared to control (CTRL) (Figure 3A). The lower bodyweight could not be attributed to a reduced food intake (Figure 3B) or an increased fecal weight (Figure 3C). Fecal lipid

excretion was significantly higher in the GG mice as compared to the CTRL mice (Figure 3C), suggesting that the lower bodyweight in the GG mice may be explained by decreased lipid absorption. Along with the lower bodyweight, weights of epididymal and mesenteric fat pads and liver were significantly lower in the GG group as compared with the CTRL group, while weight of the caecum was higher in both RS and GG groups (Figure 3D).

In line with the suppression of bodyweight gain, GG improved whole body glucose tolerance (Figure 3E), reduced fasting plasma insulin levels (Figure 3F), and attenuated immune cells infiltration in adipose tissue. Specifically, flow cytometry analysis demonstrated that the abundance of leukocytes (CD45+) and macrophages (CD45+F4/80+CD11B+) was significantly lower in the epididymal fat depot of the GG mice as compared to the CTRL mice, while the RS mice were not different (Supplemental Figure 3G-I). The decreased macrophage abundance was corroborated by decreased expression of chemoattractant protein *Mcp-1* and macrophages markers *F4/80* and *Cd68*. *Cd11c* and *Cd206* mRNA were also decreased in the GG group, suggesting lower presence of pro-inflammatory M1 macrophages and anti-inflammatory M2 macrophages, respectively (Figure 3J). Taken together, GG suppressed bodyweight gain, which was accompanied by decreased adipose tissue inflammation and improved glucose tolerance.

Modulation of the gut microbiota by guar gum is associated with reduced hepatic steatosis but enhanced hepatic inflammation

In accordance with a lower fat mass in the GG mice, hepatic lipid accumulation was significantly lower in mice fed GG, as revealed by H&E and Oil Red O stainings and quantitation of liver triglycerides (Figure 4A-C). Plasma alanine aminotransferase activity, however, was not different between the 3 groups (Figure 4D). Interestingly, despite the reduction in liver triglycerides, H&E staining showed more pronounced inflammation in

livers of GG mice, as revealed by the presence of inflammatory infiltrates (Figure 4A). Consistent with these data, elevated myeloperoxidase activity (Figure 4E) indicated a higher number of neutrophils in the livers of the GG mice. In contrast, the total macrophage abundance assessed by Cd68 staining and *Cd68* and *F4/80* expression was not different between the GG and CTRL mice (Figure 4F-G). Intriguingly, the higher expression of *Cd11c* and the lower expression of *Cd206* and the anti-inflammatory cytokine *Il-10* suggested that the macrophages present in the liver of the mice fed GG had a more pro-inflammatory phenotype (Figure 4G). To further elucidate the inflammatory status of the liver of the GG mice, whole genome expression profiling was performed. It was found that 3,722 genes were significantly altered upon GG feeding as compared to CTRL ($p < 0.01$) (Supplemental Figure 1A). Numerous immune-related pathways, including IL-8 signaling ($p = 1.05 \times 10^{-6}$) and complement system activation ($p = 7.76 \times 10^{-7}$), were altered in the livers of the GG mice, as determined by Ingenuity pathway analysis (Supplemental Figure 1B). Together, these data demonstrate that although feeding GG suppressed diet-induced obesity, it stimulated specific inflammatory cells and pathways in liver, whereas RS had no effect.

Modulation of the gut microbiota by guar gum is associated with enhanced hepatic fibrosis

Strikingly, further study revealed that livers of the mice fed GG exhibited pronounced features of hepatic fibrosis. Sirius Red staining showed enhanced collagen deposition in the GG mice as compared with CTRL and RS mice (Figure 5A). Likewise, hepatic stellate cell activation as visualized by α SMA immunostaining and 4-hydroxyproline content were also increased in the GG mice (Figure 5B-C). Expression profiling followed by Ingenuity pathway analysis pointed to hepatic fibrosis/hepatic stellate cell activation as the most significantly regulated pathway ($p = 7.94 \times 10^{-11}$), which was illustrated by the differential expression of numerous genes involved hepatic fibrosis and hepatic stellate cell activation (Figure 5D).

Genes highly induced in livers of GG mice included various collagens and genes involved in regulation of extracellular matrix turnover (*Timp2*) and TGF β signaling (*Tgfb1*). Elevated expression of fibrosis-related genes was corroborated by qPCR (Figure 5E). Finally, TIMP1 protein levels were elevated in livers of GG mice (Figure 5F). These data indicate that feeding GG not only increased hepatic inflammation but also promoted more advanced features of NASH i.e. liver fibrosis.

Modulation of the gut microbiota by guar gum is associated with altered levels of gut-derived metabolites

To explore the possible mechanisms linking changes in gut microbiota composition to the observed liver pathology, we focused our attention on several microbial compounds that have been proposed to mediate the effects of the gut bacteria on host metabolism, including the pro-inflammatory LPS and ethanol, and the anti-inflammatory short-chain fatty acids (SCFA)(43). Plasma levels of LPS were comparable between the GG mice and CTRL mice (Figure 6A), while ethanol levels in cecum and colon were decreased in the GG group (Figure 6B-C). With respect to the SCFA, in the cecum, the concentration of propionate was increased in both dietary fiber groups, whereas the butyrate concentration was only elevated in the GG group (Figure 6B). In the colon, GG but not RS significantly elevated acetate, propionate and butyrate concentrations as compared to CTRL (Figure 6C). In short, the observed changes in NAFLD phenotype in the GG mice are unlikely to be mediated by LPS, ethanol, or SCFAs.

Interestingly, plasma levels of the gut-derived metabolites trimethylamine (TMA)—a product of microbial conversion of choline—and trimethylamine N-oxide (TMAO), which is synthesized from TMA in the liver, were both significantly increased by GG, while RS had no effect (Figure 6D). Previously, TMAO was causally implicated in atherosclerosis and kidney fibrosis(9, 44, 45).

Accordingly, to investigate if the elevated plasma TMAO levels may contribute to the NAFLD phenotype, mice were fed the HFCFD diet with or without 0.2% TMAO (w/w) for 18 weeks. 18 weeks of TMAO feeding did not affect final bodyweight (Figure 6E). Although serum and urinary TMAO levels were about 15-fold higher in the mice fed the TMAO-enriched diet (Figure 6F), provision of TMAO did not affect hepatic steatosis, inflammation, or fibrosis, as indicated by measurement of liver triglycerides (Figure 6G), serum alanine aminotransferase activity (Figure 6H), the expression of inflammatory and fibrosis-related genes (Figure 6I-J), H&E staining (Figure 6K), and Sirius Red stainings (Figure 6L).

Another potential candidate linking changes in gut bacteria to NAFLD are the bile acids. Strikingly, total plasma bile acid levels were nearly 4-fold higher in the GG than the CTRL mice, whereas they remained unchanged in the RS mice (Figure 7A). Specifically, plasma levels of various primary bile acids including cholic acid, taurocholic acid, muricholic acids and taumuricholic acids, as well as the secondary bile acids deoxycholic acid, taurodeoxycholic acid, ursodeoxycholic acid, hyodeoxycholic acid and taurohyodeoxycholic acid were significantly higher in the GG mice as compared with CTRL mice (Figure 7A). Moreover, total bile acid levels in the liver were also increased in the GG mice as compared with the CTRL mice (Figure 7B). The higher plasma and hepatic bile acid levels were accompanied by elevated hepatic expression of the FXR target *Slc51b* and a compensatory downregulation of *Cyp7a1* and *Cyp8b1* (Figure 7C), enzymes involved in bile acid synthesis, and *Ntcp* (*Slc10a1*), a bile salt importer (Figure 7D). No change was observed in the expression of the bile acid exporter *Bsep* (*Abcb11*) (Figure 7D). Interestingly, levels of bile acids in the feces were significantly lower in the GG mice (Figure 7E), concomitant with reduced ileal expression of *Fgf15* and elevated expression of the ileal bile acid transporter *Asbt* (*Slc10a2*) and *Slc51b* (Figure 7F). Together, these data suggest that GG enhanced bile

acid absorption, leading to higher bile acid levels in the plasma and elevated bile acid content in the liver, which in turn triggered compensatory changes in expression of genes involved in hepatic bile acid synthesis and uptake.

To examine if the elevated plasma levels of bile acids may contribute to hepatic inflammation and fibrosis, we gave mice the bile acid taurocholic acid for 7 days mixed it in their feed (0.5% (wt/wt)). Provision of taurocholic acid raised plasma taurocholic acid levels by 40-fold as compared to CTRL (Figure 8A). In addition, taurocholic acid also significantly increased the primary bile acids cholic acid, glycocholic acid, chenodeoxycholic acid, taurochenodeoxycholic acid and unconjugated muricholic acids, as well as the secondary bile acids deoxycholic acid, taurodeoxycholic acid, glycodeoxycholic acid, ursodeoxycholic acid and ω -muricholic acid (Figure 8A). The higher plasma bile acid levels were associated with compensatory downregulation of *Cyp7a1*, *Cyp27a1*, *Cyp8b1* and *Ntcp* and upregulation of *Slc51b* in liver (Figure 8B-C). Importantly, provision of taurocholic acid markedly increased plasma alanine aminotransferase activity (Figure 8D), upregulated the expression of inflammatory genes (Figure 8E), and stimulated leukocyte infiltration (Figure 8F). Moreover, taurocholic acid promoted hepatic fibrosis as revealed by elevated expression of the fibrosis markers collagen type I alpha 1 and *Timp1* (Figure 8G), and enhanced collagen deposition (Figure 8H). Analysis of a publicly available transcriptomics dataset (GSE34730) of livers of mice treated with cholic acid or deoxycholic acid for 2 weeks confirmed the marked stimulatory effect of oral administration of bile acids on genes implicated in hepatic inflammation and fibrosis. Specifically, Ingenuity pathway analysis showed the significant induction of numerous pathways related to immune cells and cytokines signaling, including IL-8 signaling and acute phase response signaling, as well as hepatic fibrosis/hepatic stellate activation. These effects were similarly observed in conventionalized and germ-free mice, indicating that the effects of oral cholic and deoxycholic acid on liver inflammation and

fibrosis is not dependent on bacterial conversion (Supplemental Figure 2). Together, these data suggest that elevated plasma levels of bile acids can lead to hepatic inflammation and fibrosis in mice fed GG.

Suppression of the gut bacteria by oral antibiotics attenuates NAFLD development

In order to determine the direct impact of the gut microbiota on features of NAFLD, mice fed the HFCFD diet were given antibiotics via the drinking water for the entire duration of the dietary intervention. Oral administration of antibiotics led to a large increase in the weight of the cecum (Figure 9A), and caused a massive decrease in DNA levels in the feces (Figure 9B). In addition, levels of 16s rRNA were dramatically reduced in the feces (Figure 9C), as was observed for SCFA levels in the cecum (Figure 9D), demonstrating the effective suppression of the bacteria in the colon. Interestingly, antibiotics triggered an outgrowth of fungi (Figure 9C). At the end of the dietary intervention, final bodyweights were similar between the antibiotic-treated and control mice (Figure 9E). Antibiotics treatment did not affect hepatic steatosis development, as indicated by quantitative measurement of liver triglycerides (Figure 9F) and H&E staining (Figure 9G).

Strikingly, oral antibiotic caused a marked decrease in serum ALT activity (Figure 10A), as well as a decrease in the expression of inflammatory markers in the liver (Figure 10B). In addition, antibiotics treatment reduced hepatic fibrosis as indicated by markedly lower expression of the fibrosis markers collagen type I alpha 1, α SMA and *Timp1* (Figure 10C), and less collagen deposition (Figure 10D). While LPS levels in portal blood were not different between control and antibiotic-treated mice (Figure 10E), antibiotics treatment led to a non-significant reduction in the portal concentration of primary bile acids and a highly significant 10-fold reduction in the concentration of secondary bile acids (Figure 10F), hinting at a potential role of bile acids in the attenuation of features of NAFLD in the livers of the

antibiotic-treated mice. Specifically, in the portal blood the primary bile acids cholic acid, chenodeoxycholic acid and muricholic acids and almost all secondary bile acids were reduced upon antibiotics treatment (Figure 10G). The reduction in portal delivery of bile acids was accompanied by a significant reduction in hepatic expression of the FXR target *Slc51b* and a compensatory induction of genes involved in bile acids synthesis, including *Cyp7a1*, *Cyp27a1*, and *Cyp8b1*, as well as the bile acid importer *Ntcp* and exporter *Bsep* (Figure 10H-I). Surprisingly, total bile acid levels were increased in the livers of antibiotic-treated mice (Figure 10J). As expected, treatment with antibiotics caused a marked reduction in fecal excretion of secondary bile acid levels, whereas excretion of primary bile acids remained unchanged (Figure 10K). Together, these data indicate that suppression of the gut bacteria attenuates features of NAFLD, possibly via reduced portal delivery of bile acids.

Discussion

Emerging evidence points to an association between the gut microbiota and NAFLD (46). However, data on an actual causal role of the gut microbiota in NAFLD are very scarce. Here we found that stimulation of the gut microbiota using guar gum promoted liver inflammation and fibrosis. Inasmuch as guar gum is a pre-biotic non-digestible carbohydrate and is thus expected to act exclusively via its fermentation by the gut bacteria, our results suggest a direct impact of the gut microbiota on the pathogenesis of NAFLD. By contrast, suppression of the gut bacteria using oral antibiotics attenuated liver inflammation and fibrosis. The effects of microbial modulation by guar gum could be linked to altered circulating and hepatic levels of bile acids, which were shown to induce features of hepatic inflammation and fibrosis. Our data thus suggest that the gut bacteria may be able to influence NAFLD via bile acids.

It should be noted that the stimulation of hepatic inflammation and fibrosis by guar gum was unrelated to obesity—an important causal factor of NAFLD—as guar gum suppressed diet-induced weight gain and concomitant glucose intolerance and adipose tissue inflammation. In contrast to guar gum, resistant starch did not have any impact on NAFLD, probably due to the minor effect of resistant starch on gut microbial composition and levels of fermentation products (47).

Ideally, feeding guar gum should be combined with the use of antibiotics, thereby allowing direct investigation of the role of the gut microbiota in the effects of guar gum. However, in our experience it is impossible to combine the use of antibiotics with feeding a diet enriched in dietary fiber. Specifically, we found that giving mice antibiotics while on a high fiber diet quickly led to an intestinal blockage and massive weight loss, forcing us to end the experiment prematurely. This observation underscores that dietary fiber cannot be properly processed in the absence of a well-functioning gut microbiota.

Several mechanisms have been proposed to explain the link between the gut microbiota and host metabolism. These mechanisms mainly revolve around specific microbial metabolites or compounds, including lipopolysaccharide, SCFA, TMA, ethanol and bile acids, the latter of which are extensively metabolized by gut microbiota. TMA has been linked to NAFLD by reflecting the microbial conversion and depletion of choline (48). We found significantly higher plasma TMA levels in mice fed GG. Upon absorption, TMA is rapidly oxidized in the liver to TMAO by flavin monooxygenases. Gao *et al.* showed that dietary TMAO increases adipose tissue mRNA levels and serum levels of MCP-1 in mice (49). In addition, TMAO has also been shown to exacerbate atherosclerosis development in mice and is positively linked to cardiovascular disease risk in humans. Importantly, suppression of the gut microbiota using antibiotics lowered plasma TMAO levels and reduced atherosclerosis (9, 44). Furthermore, TMAO was also recently implicated in kidney fibrosis (45). In our study, however, elevated plasma TMAO levels did not seem to be responsible for the aggravation of NAFLD in mice fed guar gum, as feeding mice TMAO for 18 weeks had no effect on any indicators of NAFLD or fibrosis, despite markedly elevating circulating and urinary TMAO levels.

In addition to TMA and TMAO, plasma total bile acids were elevated in the GG but not RS mice. The parallel reduction in fecal bile acids suggests that bile acids are more efficiently absorbed in the mice fed guar gum. The increase in plasma bile acid levels was accompanied by elevated hepatic bile acid content and worsening of NAFLD and fibrosis. To investigate if bile acids could be causally involved in the progression of NAFLD upon guar gum feeding, mice were fed chow supplemented with taurocholic acid. Taurocholic acid feeding increased plasma levels of a range of different bile acids, which was associated with activation of specific features of NAFLD. These data suggest that elevated plasma and hepatic bile acids are a plausible mechanistic link between changes in gut microbial composition in mice fed guar gum and worsening of NAFLD. Consistent with this hypothesis, hepatic bile acid levels

were found to be elevated in humans with steatohepatitis (54). Furthermore, NAFLD was found to be associated with intestinal dysbiosis and altered fecal bile acid levels in human subjects (53).

One type of bile acid that may be particularly involved in promoting liver injury and NAFLD is deoxycholic acid, levels of which were increased by 4.2-fold in the plasma of mice fed guar gum. Recently, Yoshimoto *et al.*(55) linked increased deoxycholic acid levels upon high-fat feeding to the development of NAFLD-related hepatocellular carcinomas. Suppression of the microbiota by antibiotics lowered serum deoxycholic acid levels and mitigated hepatocellular carcinoma development, suggesting that microbial production of deoxycholic acid may have detrimental effects on the liver. The mechanism by which bile acids may promote liver injury and hepatic inflammation and fibrosis may involve enhanced leakage of tight junctions of bile duct epithelial cells causing cholangitis, as well as the activation and proliferation of periductal myofibroblasts leading to periductal fibrosis (56). Furthermore, it is well established that elevated intrahepatic bile acid levels trigger hepatocyte apoptosis, possibly leading to NASH (57–59). Future studies should address the cellular mechanism(s) by which microbiota-dependent changes in portal and hepatic bile acids may influence NAFLD.

The increase in liver bile acid content in the mice treated with antibiotics may be taken as evidence that bile acids cannot be responsible for the reduced liver injury, inflammation and fibrosis in these mice. However, it is likely that the increase in liver bile acid content reflects increased bile acid synthesis, as opposed to increased portal delivery of bile acids, which in fact was substantially decreased. It is conceivable that the newly synthesized bile acids are immediately secreted and are primarily located in the bile ducts, where they may not inflict liver injury. By contrast, the reduction in portal delivery of bile acids may lead to lower uptake of bile acids by hepatocytes, and thereby attenuate liver injury, inflammation and fibrosis.

Our results are consistent with previous studies showing that modulation of the gut microbiota influences bile acid levels and metabolism (60–62). These studies have pointed to intestinal FXR signaling and resultant changes in FGF15 and ceramides as potential intermediate between microbiota-induced changes in bile acids on the one hand, and liver triglycerides and bile acid synthesis on the other hand. Although our data are not inconsistent with a role of intestinal FXR signaling, FGF15, and ceramides, our study highlights the potential role of bile acids as causal factor in linking changes in the gut bacteria to altered liver inflammation and fibrosis.

It should be noted that in contrast to previous data (50–52), we did not find any evidence that the protective effective effect of antibiotics on the pathogenesis of NAFLD may be mediated by LPS, as portal LPS levels were not altered upon antibiotic-treatment.

In our study, specific gut microbial taxa could be linked to the transition from simple steatosis to NASH and fibrosis. The higher relative abundance of the genera *Bifidobacterium* and *Prevotella*, and of the species *Desulfovibrio C21_c20* and *Akkermansia muciniphila* as observed in the colonic luminal content of the GG mice, have not been observed in other mouse studies linking specific gut microbial taxa to the progression of NAFLD. However, these studies used either bile duct ligation(18, 63), a methionine choline-deficient diet(64) or carbon-tetrachloride injections(63) to induce liver injury. Bacteria within the genera *Lactobacillus*, *Bifidobacterium* and *Streptococcus* have been demonstrated to suppress hepatic inflammation in mice and humans(65, 66). In addition to dampening hepatic inflammation, *Lactobacillus* and *Bifidobacterium* have also been shown to reduce hepatic fibrosis(67). Furthermore, *Bifidobacterium* are known to be able to ferment guar gum (68, 69) and possess active bile salt hydrolases (70). Since unconjugated bile acids are less efficient in the solubilization and absorption of fecal lipids (70), one possible scenario is that by increasing

bile salt hydrolase activity and unconjugated bile acids, the increase in *Bifidobacterium* may be responsible for the elevated fecal lipid excretion.

Guar gum is composed of galactose and mannose residues and is extracted from the seeds of guar beans. It is mainly used as a thickening agent in several food products including ice creams, sauces and cheese spreads(71). Although we show that dietary guar gum promotes the progression of NAFLD, caution should be exercised in extrapolating these data to the human situation because, 1) the dose of guar gum used substantially exceeds the amounts ingested by humans, 2) the microbiota composition is vastly different between mice and humans. In our study, we used guar gum as a model compound to study the effect of modulating the gut microbiota composition on NAFLD.

In conclusion, we find that stimulation of the gut bacteria by guar gum leads to deleterious effects on hepatic inflammation and fibrosis in a mouse model of NAFLD, whereas suppression of the gut bacteria by antibiotics attenuates NAFLD. Overall, we provide evidence of a causal link between disturbances in gut bacteria, bile acids, and NAFLD.

Acknowledgements

We thank Dr. A.H. Mulder (Rijnstate Hospital, the Netherlands) for excellent advice with histopathological analysis and Martijn Koehorst for the bile acid measurements. This research was supported by The Netherlands Cardiovascular Research Committee IN-CONTROL grant (CVON 2012-03) and the Rembrandt Institute for Cardiovascular Research 2012. TMA and TMAO analyses were supported by grants from the National Institutes of Health and the Office of Dietary Supplements (HL103866, HL122283, and AA024333).

References

1. Finucane, M. M., G. A. Stevens, M. J. Cowan, G. Danaei, J. K. Lin, C. J. Paciorek, G. M. Singh, H. R. Gutierrez, Y. Lu, A. N. Bahalim, F. Farzadfar, L. M. Riley, and M. Ezzati. 2011. National, regional, and global trends in body-mass index since 1980: Systematic analysis of health examination surveys and epidemiological studies with 960 country-years and 9.1 million participants. *Lancet*. **377**: 557–567.
2. Ridaura, V. K., J. J. Faith, F. E. Rey, J. Cheng, A. E. Duncan, A. L. Kau, N. W. Griffin, V. Lombard, B. Henrissat, J. R. Bain, M. J. Muehlbauer, O. Ilkayeva, C. F. Semenkovich, K. Funai, D. K. Hayashi, B. J. Lyle, M. C. Martini, L. K. Ursell, J. C. Clemente, W. Van Treuren, W. a Walters, R. Knight, C. B. Newgard, A. C. Heath, and J. I. Gordon. 2013. Gut microbiota from twins discordant for obesity modulate metabolism in mice. *Science*. **341**: 1241214.
3. Vrieze, A., E. Van Nood, F. Holleman, J. Salojärvi, R. S. Kootte, J. F. W. M. Bartelsman, G. M. Dallinga-Thie, M. T. Ackermans, M. J. Serlie, R. Oozeer, M. Derrien, A. Druesne, J. E. T. Van Hylckama Vlieg, V. W. Bloks, A. K. Groen, H. G. H. J. Heilig, E. G. Zoetendal, E. S. Stroes, W. M. de Vos, J. B. L. Hoekstra, and M. Nieuwdorp. 2012. Transfer of intestinal microbiota from lean donors increases insulin sensitivity in individuals with metabolic syndrome. *Gastroenterology*. **143**: 913–6.
4. Lam, Y. Y., C. W. Y. Ha, C. R. Campbell, A. J. Mitchell, A. Dinudom, J. Oscarsson, D. I. Cook, N. H. Hunt, I. D. Caterson, A. J. Holmes, and L. H. Storlien. 2012. Increased gut permeability and microbiota change associate with mesenteric fat inflammation and metabolic dysfunction in diet-induced obese mice. *PLoS One*. **7**: e34233.
5. Janssen, A. W. F., and S. Kersten. 2015. The role of the gut microbiota in metabolic health. *FASEB J*. **29**: 3111–3123.
6. Sommer, F., and F. Bäckhed. 2013. The gut microbiota--masters of host development and

- physiology. *Nat. Rev. Microbiol.* **11**: 227–38.
7. Clemente, J. C., L. K. Ursell, L. W. Parfrey, and R. Knight. 2012. The impact of the gut microbiota on human health: An integrative view. *Cell.* **148**: 1258–1270.
 8. Biedermann, L., and G. Rogler. 2015. The intestinal microbiota: its role in health and disease. *Eur. J. Pediatr.* **174**: 151–167.
 9. Wang, Z., E. Klipfell, B. J. Bennett, R. Koeth, B. S. Levison, B. Dugar, A. E. Feldstein, E. B. Britt, X. Fu, Y.-M. Chung, Y. Wu, P. Schauer, J. D. Smith, H. Allayee, W. H. W. Tang, J. a DiDonato, A. J. Lusis, and S. L. Hazen. 2011. Gut flora metabolism of phosphatidylcholine promotes cardiovascular disease. *Nature.* **472**: 57–63.
 10. Janssen, A. W. F., and S. Kersten. 2017. Potential mediators linking gut bacteria to metabolic health: a critical view. *J. Physiol.* **595**: 477–487.
 11. Schuppan, D., and J. M. Schattenberg. 2013. Non-alcoholic steatohepatitis: pathogenesis and novel therapeutic approaches. *J. Gastroenterol. Hepatol.* **28 Suppl 1**: 68–76.
 12. Tilg, H., and A. R. Moschen. 2010. Evolution of inflammation in nonalcoholic fatty liver disease: The multiple parallel hits hypothesis. *Hepatology.* **52**: 1836–1846.
 13. Nassir, F., and J. Ibdah. 2014. Role of mitochondria in nonalcoholic fatty liver disease. *Int. J. Mol. Sci.* **15**: 8713–8742.
 14. Jiang, W., N. Wu, X. Wang, Y. Chi, Y. Zhang, X. Qiu, Y. Hu, J. Li, and Y. Liu. 2015. Dysbiosis gut microbiota associated with inflammation and impaired mucosal immune function in intestine of humans with non-alcoholic fatty liver disease. *Sci. Rep.* **5**: 1–7.
 15. Mouzaki, M., E. M. Comelli, B. M. Arendt, J. Bonengel, S. K. Fung, S. E. Fischer, I. D. Mcgilvray, and J. P. Allard. 2013. Intestinal microbiota in patients with nonalcoholic fatty liver disease. *Hepatology.* **58**: 120–127.
 16. Jiang, C., C. Xie, F. Li, L. Zhang, R. G. Nichols, K. W. Krausz, J. Cai, Y. Qi, Z. Fang, S.

- Takahashi, N. Tanaka, D. Desai, S. G. Amin, I. Albert, A. D. Patterson, and F. J. Gonzalez. 2015. Intestinal farnesoid X receptor signaling promotes nonalcoholic fatty liver disease. *J. Clin. Invest.* **125**: 386–402.
17. Henao-Mejia, J., E. Elinav, C. Jin, L. Hao, W. Z. Mehal, T. Strowig, C. a Thaiss, A. L. Kau, S. C. Eisenbarth, M. J. Jurczak, J.-P. Camporez, G. I. Shulman, J. I. Gordon, H. M. Hoffman, and R. a Flavell. 2012. Inflammasome-mediated dysbiosis regulates progression of NAFLD and obesity. *Nature.* **482**: 179–85.
18. De Minicis, S., C. Rychlicki, L. Agostinelli, S. Saccomanno, C. Candelaresi, L. Trozzi, E. Mingarelli, B. Facinelli, G. Magi, C. Palmieri, M. Marzioni, A. Benedetti, and G. Svegliati-Baroni. 2014. Dysbiosis contributes to fibrogenesis in the course of chronic liver injury in mice. *Hepatology.* **59**: 1738–1749.
19. Nomura, K., and T. Yamanouchi. 2012. The role of fructose-enriched diets in mechanisms of nonalcoholic fatty liver disease. *J. Nutr. Biochem.* **23**: 203–8.
20. Song, P., Y. Zhang, and C. D. Klaassen. 2011. Dose-response of five bile acids on serum and liver bile acid concentrations and hepatotoxicity in mice. *Toxicol. Sci.* **123**: 359–367.
21. Rakoff-Nahoum, S., J. Paglino, F. Eslami-Varzaneh, S. Edberg, and R. Medzhitov. 2004. Recognition of commensal microflora by toll-like receptors is required for intestinal homeostasis. *Cell.* **118**: 229–241.
22. Bieghs, V., K. Wouters, P. J. van Gorp, M. J. J. Gijbels, M. P. J. de Winther, C. J. Binder, D. Lütjohann, M. Febbraio, K. J. Moore, M. van Bilsen, M. H. Hofker, and R. Shiri-Sverdlov. 2010. Role of Scavenger Receptor A and CD36 in Diet-Induced Nonalcoholic Steatohepatitis in Hyperlipidemic Mice. *Gastroenterology.* **138**: 2477–2486.
23. Nagy, R. A., A. P. A. van Montfoort, A. Dijkers, J. van Echten-Arends, I. Homminga, J.

- A. Land, A. Hoek, and U. J. F. Tietge. 2015. Presence of bile acids in human follicular fluid and their relation with embryo development in modified natural cycle IVF. *Hum. Reprod.* **30**: 1102–1109.
24. Wang, Z., B. S. Levison, J. E. Hazen, L. Donahue, X. M. Li, and S. L. Hazen. 2014. Measurement of trimethylamine-N-oxide by stable isotope dilution liquid chromatography tandem mass spectrometry. *Anal. Biochem.* **455**: 35–40.
25. Koeth, R. A., B. S. Levison, M. K. Culley, J. A. Buffa, Z. Wang, J. C. Gregory, E. Org, Y. Wu, L. Li, J. D. Smith, W. H. W. Tang, J. A. DiDonato, A. J. Lusis, and S. L. Hazen. 2014. γ -Butyrobetaine Is a Proatherogenic Intermediate in Gut Microbial Metabolism of L-Carnitine to TMAO. *Cell Metab.* **20**: 799–812.
26. Govers, M. J., and R. Van der Meet. 1993. Effects of dietary calcium and phosphate on the intestinal interactions between calcium, phosphate, fatty acids, and bile acids. *Gut.* **34**: 365–370.
27. van Meer, H., G. Boehm, F. Stellaard, A. Vriesema, J. Knol, R. Havinga, P. J. Sauer, and H. J. Verkade. 2008. Prebiotic oligosaccharides and the enterohepatic circulation of bile salts in rats. *Am. J. Physiol. Gastrointest. Liver Physiol.* **294**: G540–G547.
28. Bolstad, B. M., R. A. Irizarry, M. Åstrand, and T. P. Speed. 2003. A comparison of normalization methods for high density oligonucleotide array data based on variance and bias. *Bioinformatics.* **19**: 185–193.
29. Irizarry, R. A., B. M. Bolstad, F. Collin, L. M. Cope, B. Hobbs, and T. P. Speed. 2003. Summaries of Affymetrix GeneChip probe level data. *Nucleic Acids Res.* **31**: e15.
30. Dai, M., P. Wang, A. D. Boyd, G. Kostov, B. Athey, E. G. Jones, W. E. Bunney, R. M. Myers, T. P. Speed, H. Akil, S. J. Watson, and F. Meng. 2005. Evolving gene/transcript definitions significantly alter the interpretation of GeneChip data. *Nucleic Acids Res.* **33**: 1–9.

31. Sartor, M. a, C. R. Tomlinson, S. C. Wesselkamper, S. Sivaganesan, G. D. Leikauf, and M. Medvedovic. 2006. Intensity-based hierarchical Bayes method improves testing for differentially expressed genes in microarray experiments. *BMC Bioinformatics*. **7**: 538.
32. Storey, J. D., and R. Tibshirani. 2003. Statistical significance for genomewide studies. *Proc. Natl. Acad. Sci. U. S. A.* **100**: 9440–9445.
33. Jamall, I. S., V. N. Finelli, and S. S. Que Hee. 1981. A simple method to determine nanogram levels of 4-hydroxyproline in biological tissues. *Anal. Biochem.* **112**: 70–75.
34. Gevers, D., S. Kugathasan, L. A. Denson, Y. Vázquez-Baeza, W. Van Treuren, B. Ren, E. Schwager, D. Knights, S. J. Song, M. Yassour, X. C. Morgan, A. D. Kostic, C. Luo, A. González, D. McDonald, Y. Haberman, T. Walters, S. Baker, J. Rosh, M. Stephens, M. Heyman, J. Markowitz, R. Baldassano, A. Griffiths, F. Sylvester, D. Mack, S. Kim, W. Crandall, J. Hyams, C. Huttenhower, R. Knight, and R. J. Xavier. 2014. The treatment-naive microbiome in new-onset Crohn’s disease. *Cell Host Microbe*. **15**: 382–392.
35. Caporaso, J. G., J. Kuczynski, J. Stombaugh, K. Bittinger, F. D. Bushman, E. K. Costello, N. Fierer, A. G. Peña, J. K. Goodrich, J. I. Gordon, G. a Huttley, S. T. Kelley, D. Knights, J. E. Koenig, R. E. Ley, C. a Lozupone, D. Mcdonald, B. D. Muegge, M. Pirrung, J. Reeder, J. R. Sevinsky, P. J. Turnbaugh, W. a Walters, J. Widmann, T. Yatsunenko, J. Zaneveld, and R. Knight. 2010. QIIME allows analysis of high-throughput community sequencing data. *Nat. Methods*. **7**: 335–336.
36. Segata, N., J. Izard, L. Waldron, D. Gevers, L. Miropolsky, W. S. Garrett, and C. Huttenhower. 2011. Metagenomic biomarker discovery and explanation. *Genome Biol.* **12**: R60.
37. Suzuki, M. T., L. T. Taylor, and E. F. DeLong. 2000. Quantitative analysis of small-

- subunit rRNA genes in mixed microbial populations via 5'-nuclease assays. *Appl. Environ. Microbiol.* **66**: 4605–4614.
38. Pryce, T. M., S. Palladino, I. D. Kay, and G. W. Coombs. 2003. Rapid identification of fungi by sequencing the ITS1 and ITS2 regions using an automated capillary electrophoresis system. *Med. Mycol.* **41**: 369–381.
39. Haenen, D., C. Souza, J. Zhang, S. J. Koopmans, G. Bosch, J. Vervoort, W. J. J. Gerrits, B. Kemp, H. Smidt, and M. Mu. 2013. Resistant Starch Induces Catabolic but Suppresses Immune and Cell Division Pathways and Changes the Microbiome in the Proximal Colon of Male Pigs. *J. Nutr.* **143**: 1889–1898.
40. Charlton, M., a. Krishnan, K. Viker, S. Sanderson, S. Cazanave, a. McConico, H. Masuoko, and G. Gores. 2011. Fast food diet mouse: novel small animal model of NASH with ballooning, progressive fibrosis, and high physiological fidelity to the human condition. *AJP Gastrointest. Liver Physiol.* **301**: G825–G834.
41. Kawanishi, N., H. Yano, T. Mizokami, M. Takahashi, E. Oyanagi, and K. Suzuki. 2012. Exercise training attenuates hepatic inflammation, fibrosis and macrophage infiltration during diet induced-obesity in mice. *Brain. Behav. Immun.* **26**: 931–41.
42. Savard, C., E. V Tartaglione, R. Kuver, W. G. Haigh, G. C. Farrell, S. Subramanian, A. Chait, M. M. Yeh, L. S. Quinn, and G. N. Ioannou. 2013. Synergistic interaction of dietary cholesterol and dietary fat in inducing experimental steatohepatitis. *Hepatology.* **57**: 81–92.
43. Bashiardes, S., H. Shapiro, S. Rozin, O. Shibolet, and E. Elinav. 2016. Non-alcoholic fatty liver and the gut microbiota. *Mol. Metab.* **5**: 782–794.
44. Koeth, R. A., Z. Wang, B. S. Levison, J. a Buffa, E. Org, B. T. Sheehy, E. B. Britt, X. Fu, Y. Wu, L. Li, J. D. Smith, J. a DiDonato, J. Chen, H. Li, G. D. Wu, J. D. Lewis, M. Warrier, J. M. Brown, R. M. Krauss, W. H. W. Tang, F. D. Bushman, A. J. Lysis, and

- S. L. Hazen. 2013. Intestinal microbiota metabolism of L-carnitine, a nutrient in red meat, promotes atherosclerosis. *Nat. Med.* **19**: 576–85.
45. Tang, W. H. W., Z. Wang, D. J. Kennedy, Y. Wu, J. a. Buffa, B. Agatsuma-Boyle, X. S. Li, B. S. Levison, and S. L. Hazen. 2015. Gut Microbiota-Dependent Trimethylamine N-Oxide (TMAO) Pathway Contributes to Both Development of Renal Insufficiency and Mortality Risk in Chronic Kidney Disease. *Circ. Res.* **116**: 448–455.
46. Lau, E., D. Carvalho, and P. Freitas. 2015. Gut Microbiota: Association with NAFLD and Metabolic Disturbances. *Biomed Res. Int.* **2015**.
47. Lange, K., F. Hugenholtz, M. C. Jonathan, H. a Schols, M. Kleerebezem, H. Smidt, M. Müller, and G. J. E. J. Hooiveld. 2015. Comparison of the effects of five dietary fibers on mucosal transcriptional profiles, and luminal microbiota composition and SCFA concentrations in murine colon. *Mol. Nutr. Food Res.* **59**: 1590–1602.
48. Dumas, M.-E., R. H. Barton, A. Toye, O. Cloarec, C. Blancher, A. Rothwell, J. Fearnside, R. Tatoud, V. Blanc, J. C. Lindon, S. C. Mitchell, E. Holmes, M. I. McCarthy, J. Scott, D. Gauguier, and J. K. Nicholson. 2006. Metabolic profiling reveals a contribution of gut microbiota to fatty liver phenotype in insulin-resistant mice. *Proc. Natl. Acad. Sci. U. S. A.* **103**: 12511–12516.
49. Gao, X., X. Liu, J. Xu, C. Xue, Y. Xue, and Y. Wang. 2014. Dietary trimethylamine N-oxide exacerbates impaired glucose tolerance in mice fed a high fat diet. *J. Biosci. Bioeng.* **118**: 476–481.
50. Rahman, K., C. Desai, S. S. Iyer, N. E. Thorn, P. Kumar, Y. Liu, T. Smith, A. S. Neish, H. Li, S. Tan, P. Wu, X. Liu, Y. Yu, A. B. Farris, A. Nusrat, C. A. Parkos, and F. A. Anania. 2016. Loss of Junctional Adhesion Molecule A Promotes Severe Steatohepatitis in Mice on a Diet High in Saturated Fat, Fructose, and Cholesterol. *Gastroenterology.* **151**: 733–746.e12.

51. Carvalho, B. M., D. Guadagnini, D. M. L. Tsukumo, a a Schenka, P. Latuf-Filho, J. Vassallo, J. C. Dias, L. T. Kubota, J. B. C. Carvalheira, and M. J. a Saad. 2012. Modulation of gut microbiota by antibiotics improves insulin signalling in high-fat fed mice. *Diabetologia*. **55**: 2823–34.
52. Douhara, A., K. Moriya, H. Yoshiji, R. Noguchi, T. Namisaki, M. Kitade, K. Kaji, Y. Aihara, N. Nishimura, K. Takeda, Y. Okura, H. Kawaratani, and H. Fukui. 2015. Reduction of endotoxin attenuates liver fibrosis through suppression of hepatic stellate cell activation and remission of intestinal permeability in a rat non-alcoholic steatohepatitis model. *Mol. Med. Rep.* **11**: 1693–1700.
53. Mouzaki, M., A. Y. Wang, R. Bandsma, E. M. Comelli, B. M. Arendt, L. Zhang, S. Fung, S. E. Fischer, I. G. McGilvray, and J. P. Allard. 2016. Bile Acids and Dysbiosis in Non-Alcoholic Fatty Liver Disease. *PLoS One*. **11**: e0151829.
54. Aranha, M. M., H. Cortez-Pinto, A. Costa, I. B. M. da Silva, M. E. Camilo, M. C. de Moura, and C. M. P. Rodrigues. 2008. Bile acid levels are increased in the liver of patients with steatohepatitis. *Eur. J. Gastroenterol. Hepatol.* **20**: 519–525.
55. Yoshimoto, S., T. M. Loo, K. Atarashi, H. Kanda, S. Sato, S. Oyadomari, Y. Iwakura, K. Oshima, H. Morita, M. Hattori, K. Honda, Y. Ishikawa, E. Hara, and N. Ohtani. 2013. Obesity-induced gut microbial metabolite promotes liver cancer through senescence secretome. *Nature*. **499**: 97–101.
56. Fickert, P., A. Fuchsbichler, H.-U. Marschall, M. Wagner, G. Zollner, R. Krause, K. Zatloukal, H. Jaeschke, H. Denk, and M. Trauner. 2006. Lithocholic acid feeding induces segmental bile duct obstruction and destructive cholangitis in mice. *Am. J. Pathol.* **168**: 410–422.
57. Woudenberg-Vrenken, T. E., L. Conde de la Rosa, M. Buist-Homan, K. N. Faber, and H. Moshage. 2013. Metformin Protects Rat Hepatocytes against Bile Acid-Induced

- Apoptosis. *PLoS One*. **8**.
58. Sodeman, T., S. F. Bronk, P. J. Roberts, H. Miyoshi, and G. J. Gores. 2000. Bile salts mediate hepatocyte apoptosis by increasing cell surface trafficking of Fas. *Am.J Physiol Gastrointest.Liver Physiol*. **278**: G992–G999.
59. Higuchi, H., S. F. Bronk, Y. Takikawa, N. Werneburg, R. Takimoto, W. El-deiry, and G. J. Gores. 2001. The Bile Acid Glycochenodeoxycholate Induces TRAIL-Receptor 2 / DR5 Expression and Apoptosis. *J. Biol. Chem*. **276**: 38610–38618.
60. Swann, J. R., E. J. Want, F. M. Geier, K. Spagou, I. D. Wilson, J. E. Sidaway, J. K. Nicholson, and E. Holmes. 2011. Systemic gut microbial modulation of bile acid metabolism in host tissue compartments. *Proc. Natl. Acad. Sci. U. S. A*. **108**: 4523–30.
61. Sayin, S. I., A. Wahlström, J. Felin, S. Jääntti, H.-U. Marschall, K. Bamberg, B. Angelin, T. Hyötyläinen, M. Orešič, and F. Bäckhed. 2013. Gut microbiota regulates bile acid metabolism by reducing the levels of tauro-beta-muricholic acid, a naturally occurring FXR antagonist. *Cell Metab*. **17**: 225–235.
62. Zhang, Y., P. B. Limalye, H. J. Renaud, and C. D. Klaassen. 2014. Effect of various antibiotics on modulation of intestinal microbiota and bile acid profile in mice. *Toxicol. Appl. Pharmacol*. **277**: 138–145.
63. Fouts, D. E., M. Torralba, K. E. Nelson, D. A. Brenner, and B. Schnabl. 2012. Bacterial translocation and changes in the intestinal microbiome in mouse models of liver disease. *J. Hepatol*. **56**: 1283–1292.
64. Henao-Mejia, J., E. Elinav, C. A. Thaiss, and R. A. Flavell. 2013. The Intestinal Microbiota in Chronic Liver Disease. *Adv. Immunol*. **117**: 73–97.
65. Li, Z., S. Yang, H. Lin, J. Huang, P. a. Watkins, A. B. Moser, C. DeSimone, X. Y. Song, and A. M. Diehl. 2003. Probiotics and antibodies to TNF inhibit inflammatory activity

- and improve nonalcoholic fatty liver disease. *Hepatology*. **37**: 343–350.
66. Eslamparast, T., H. Poustchi, F. Zamani, M. Sharafkhah, R. Malekzadeh, and A. Hekmatdoost. 2014. Synbiotic supplementation in nonalcoholic fatty liver disease : a randomized, double-blind, placebo-controlled pilot study. *Am J Clin Nutr*. **99**: 535–542.
67. Okubo, H., H. Sakoda, A. Kushiyama, M. Fujishiro, Y. Nakatsu, T. Fukushima, Y. Matsunaga, H. Kamata, T. Asahara, Y. Yoshida, O. Chonan, M. Iwashita, F. Nishimura, and T. Asano. 2013. Lactobacillus casei strain Shirota protects against nonalcoholic steatohepatitis development in a rodent model. *Am. J. Physiol. Gastrointest. Liver Physiol*. **305**: G911-8.
68. Noack, J., B. Kleessen, J. Proll, G. Dongowski, and M. Blaut. 1998. Dietary guar gum and pectin stimulate intestinal microbial polyamine synthesis in rats. *J. Nutr*. **128**: 1385–91.
69. Ohashi, Y., K. Sumitani, M. Tokunaga, N. Ishihara, T. Okubo, and T. Fujisawa. 2015. Consumption of partially hydrolysed guar gum stimulates Bifidobacteria and butyrate-producing bacteria in the human large intestine. *Benef. Microbes*. **6**: 451–455.
70. Begley, M., C. Hill, and C. G. M. Gahan. 2006. Bile Salt Hydrolase Activity in Probiotics Bile Salt Hydrolase Activity in Probiotics. *Appl. Environ. Microbiol*. **72**: 1729–1738.
71. Mudgil, D., S. Barak, and B. S. Khatkar. 2011. Guar gum: processing, properties and food applications—A Review. *J. Food Sci. Technol*. **51**: 409–418.

Figure 1

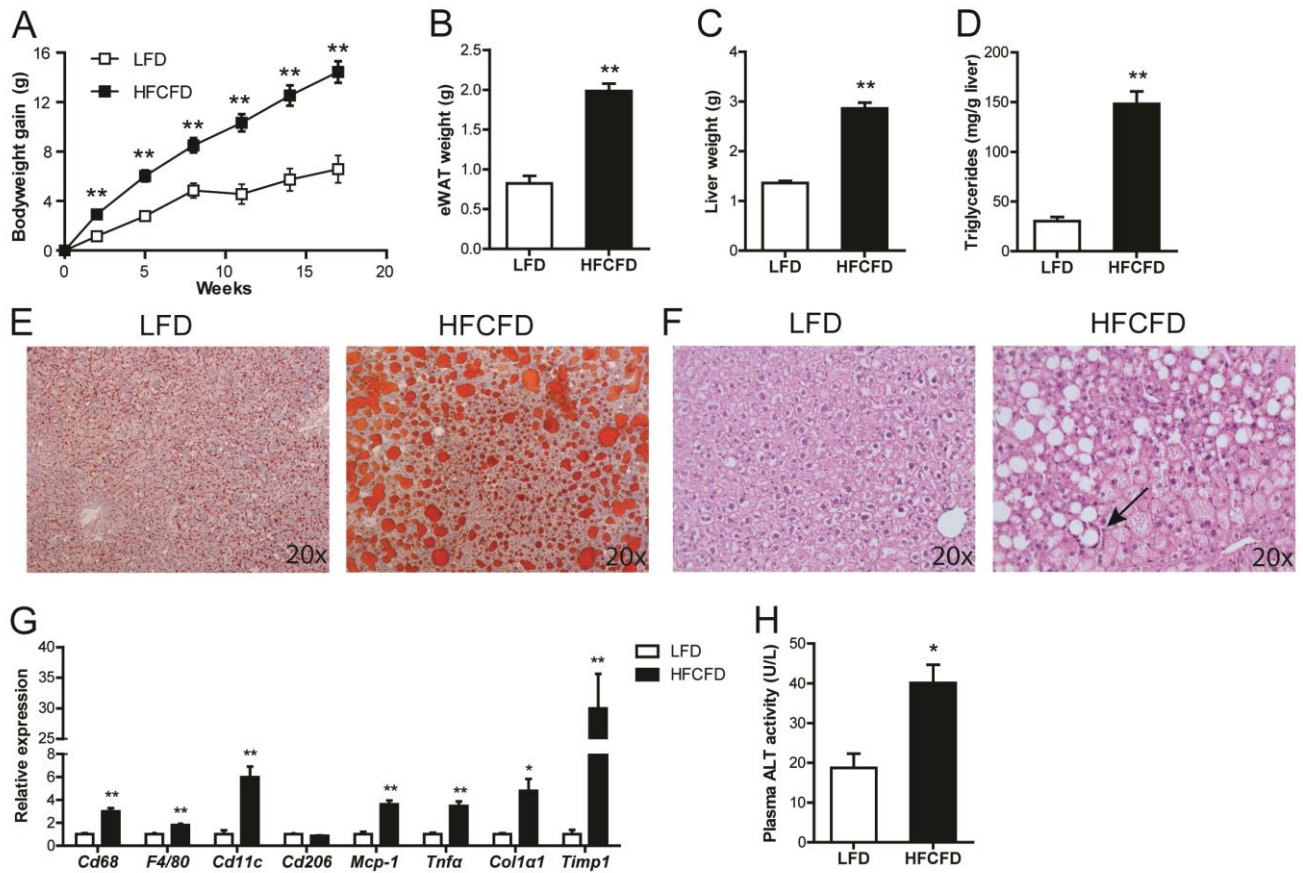


Figure 1. Effect of HFCFD on obesity and hepatic steatosis

(A) Bodyweight gain in C57Bl/6 mice fed a low fat diet or a high fat/high cholesterol/high fructose diet (HFCFD). Weight of epididymal white adipose tissue (eWAT) (B) and liver (C) after 18 weeks of dietary intervention. (D) Quantitative analysis of liver triglyceride levels. (E) Oil Red O staining and (F) H&E staining of representative liver sections. Arrow denotes inflammatory infiltrate. (G) Relative expression of inflammatory and fibrosis-related genes in the liver. Gene expression levels of mice fed low fat diet were set at 1. (H) Activity of alanine aminotransferase (ALT) in plasma. Data are presented as mean \pm SEM. Asterisks represent significant differences compared with LFD. * $p < 0.05$, ** $p \leq 0.001$.

Figure 2

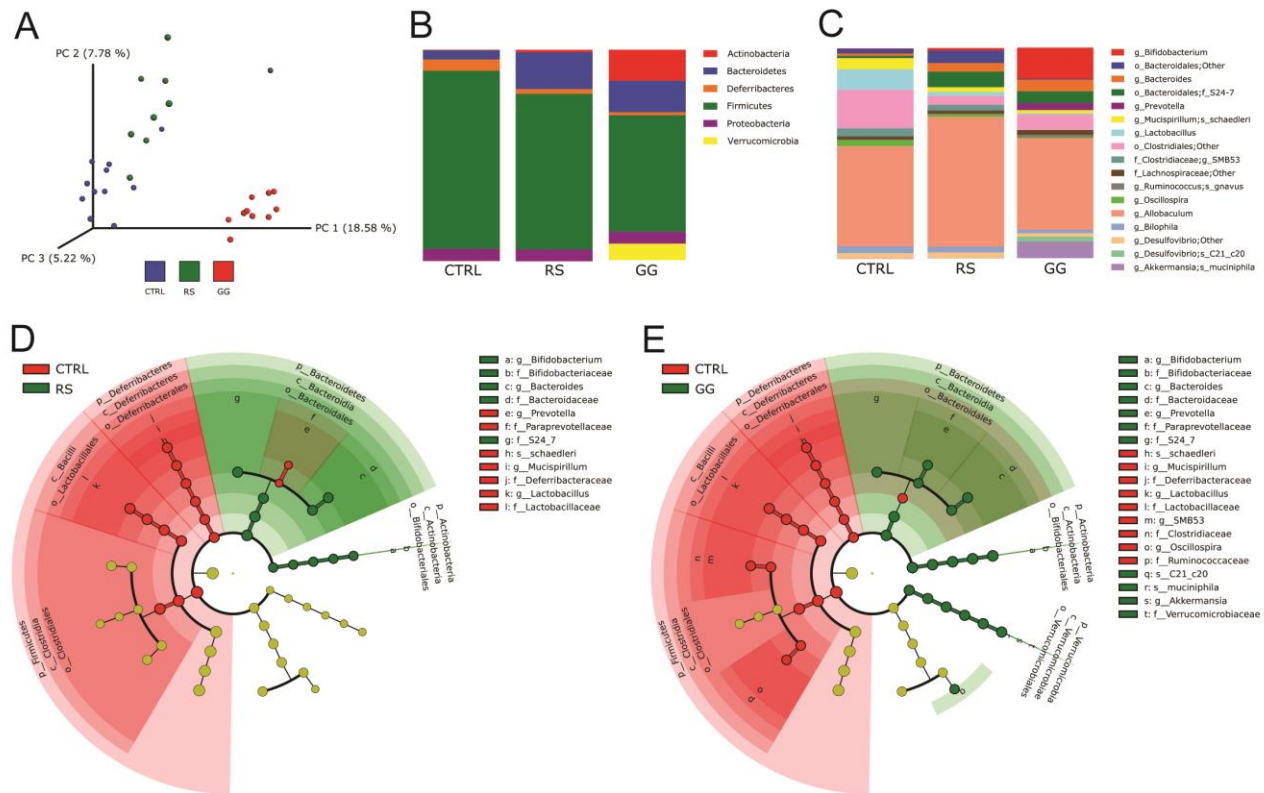


Figure 2. Guar gum alters the colonic microbial composition

(A) Principle coordinates analysis plot of unweighted UniFrac distances indicating clustering 16s rRNA gene sequences. Each circle represents an individual mouse. (B) Mean relative abundance of the predominant phyla (>0.5% in at least one of the three diet groups). (C) Mean relative abundance of bacteria reported to the lowest identifiable level. Taxonomic level is indicated by letter preceding the underscore: o, order; f, family; g, genus; s, species. (D) Cladogram representing significant enrichment of taxa in CTRL (green) or RS (red) colonic microbiota. (E) Cladogram representing significant enrichment of taxa in CTRL (green) or GG (red) colonic microbiota. The central point in the cladogram represents the domain bacteria and each ring represents the next lower taxonomic level (phylum to genus).

Figure 3

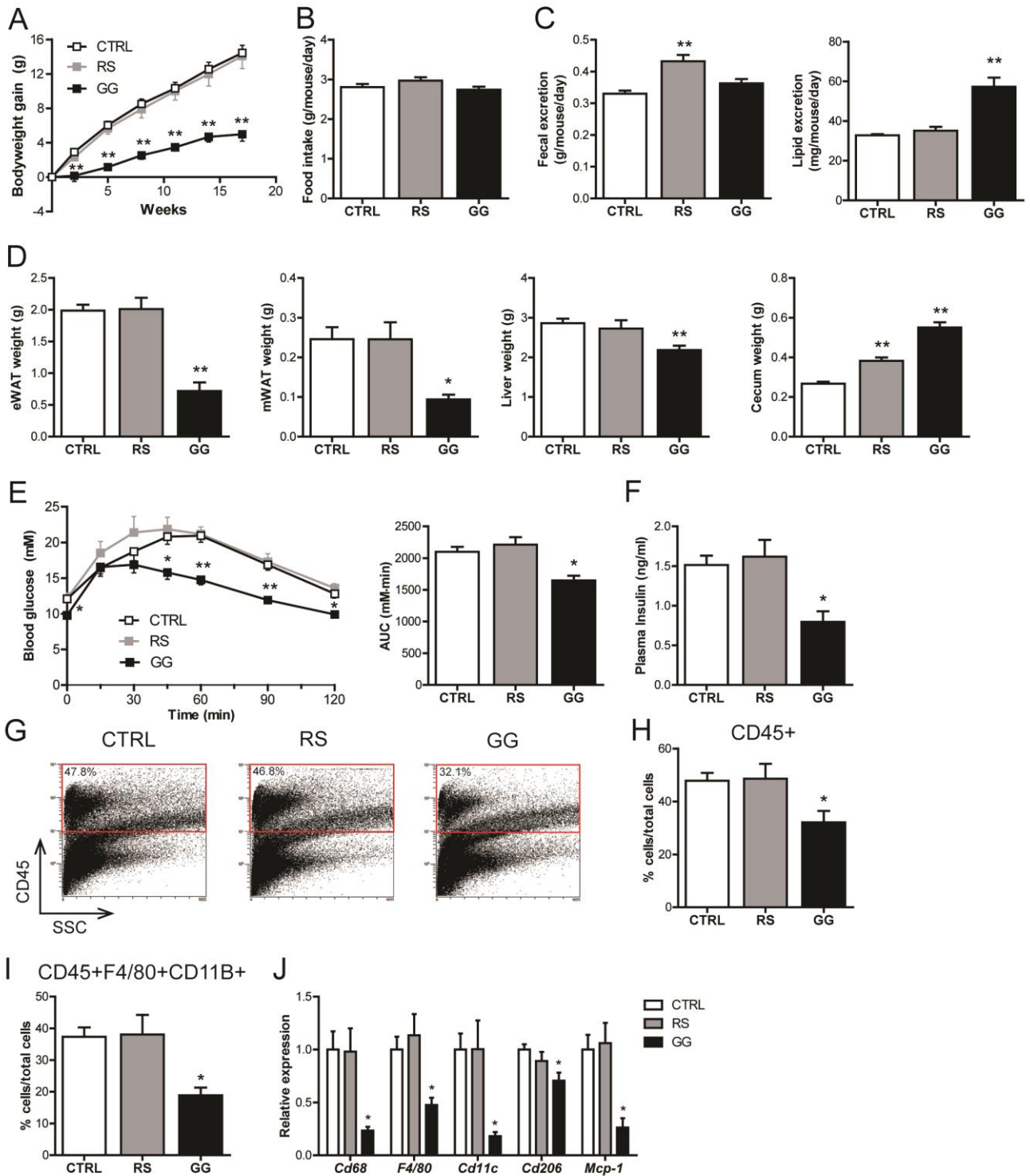


Figure 3. Stimulation of the gut microbiota by guar gum is associated with protection against the development of diet-induced obesity, improved glucose tolerance and decreased adipose tissue inflammation

(A) Changes in bodyweight in C57Bl/6 mice fed a HFCFD (CTRL) or a HFCFD supplemented with RS or GG. (B) Mean food intake per day during dietary intervention. (C) Mean fecal and lipid excretion per mouse per day in the sixth week of dietary intervention. (D) Weight of epididymal white adipose tissue (eWAT), mesenteric white adipose tissue (mWAT), liver and cecum after 18 weeks of dietary intervention. (E) Plasma glucose levels of CTRL, RS and GG mice following an intraperitoneal glucose tolerance test (GTT) and areas under the curve (AUC) after 17 weeks of dietary intervention. (F) Plasma insulin concentration after 5 hours of fasting. (G) Representative flow cytometry plots and (H) corresponding quantitative analysis of infiltrated leukocytes (CD45+) in epididymal white adipose tissue (eWAT). (I) Quantitative analysis of macrophages (F4/80+CD11B+). (J) Relative expression of inflammatory genes in eWAT. Gene expression levels in CTRL mice were set at 1. Data are presented as mean \pm SEM. Asterisks represent significant differences compared with CTRL. * p <0.05 ** p <0.001.

Figure 4

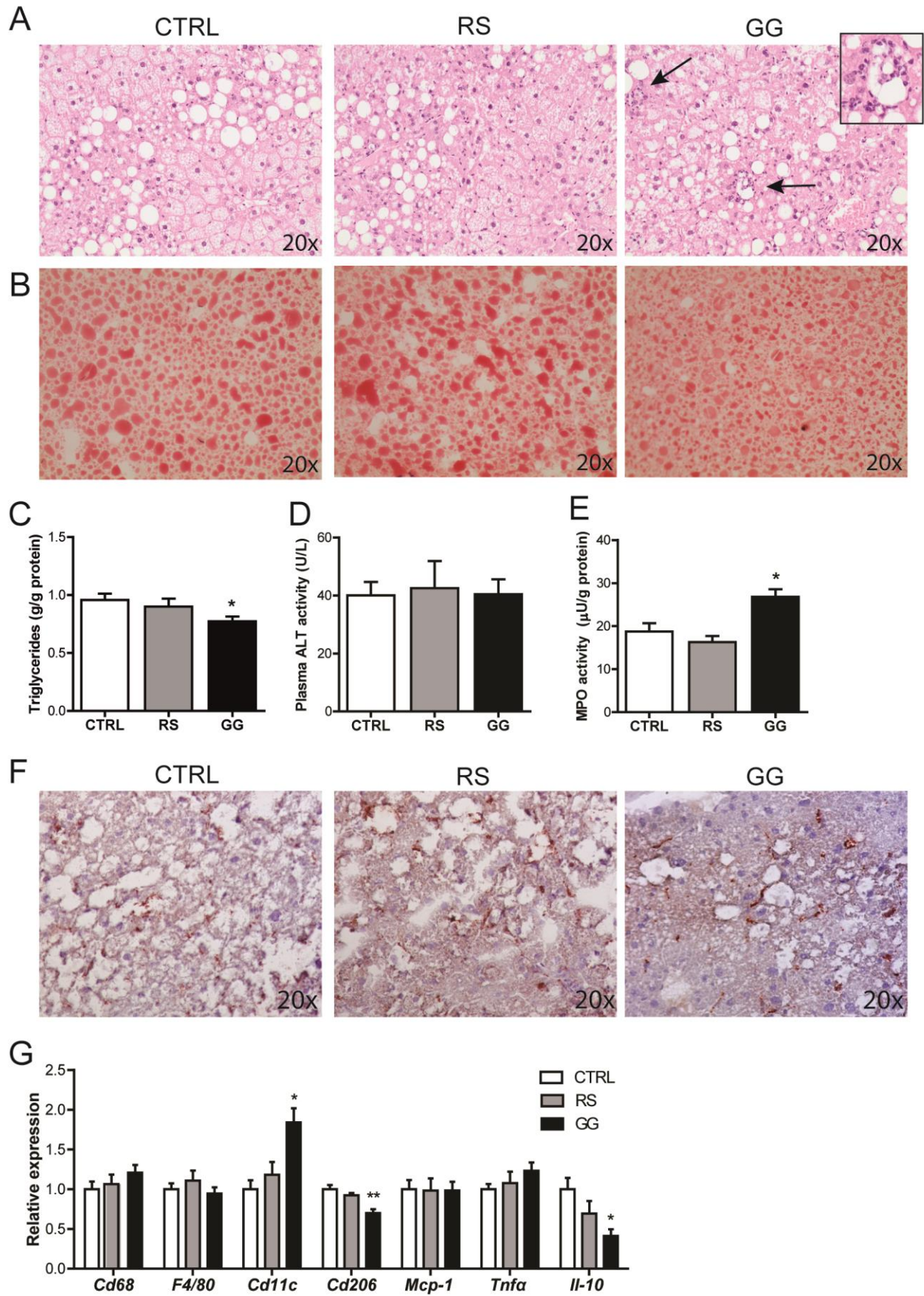


Figure 4. Stimulation of the gut microbiota by guar gum is associated with reduced hepatic steatosis but enhanced hepatic inflammation

(A) H&E staining of representative liver sections. Arrows denote inflammatory infiltrate and inset a higher magnification of the inflammatory infiltrate as observed in the livers of the GG mice. (B) Representative pictures of Oil Red O staining of liver sections. (C) Quantitative analysis of liver triglyceride levels. (D) Activity of alanine aminotransferase (ALT) in plasma. Data are presented as mean \pm SEM. (E) Liver myeloperoxidase (MPO) activity representing hepatic neutrophil content. (F) Representative pictures of liver sections stained for the macrophage marker Cd68. (G) Relative expression of inflammatory genes in the liver. Gene expression levels in CTRL mice were set at 1. Data are presented as mean \pm SEM. Asterisks represent significant differences compared with CTRL.

* $p < 0.05$, ** $p < 0.001$.

Figure 5

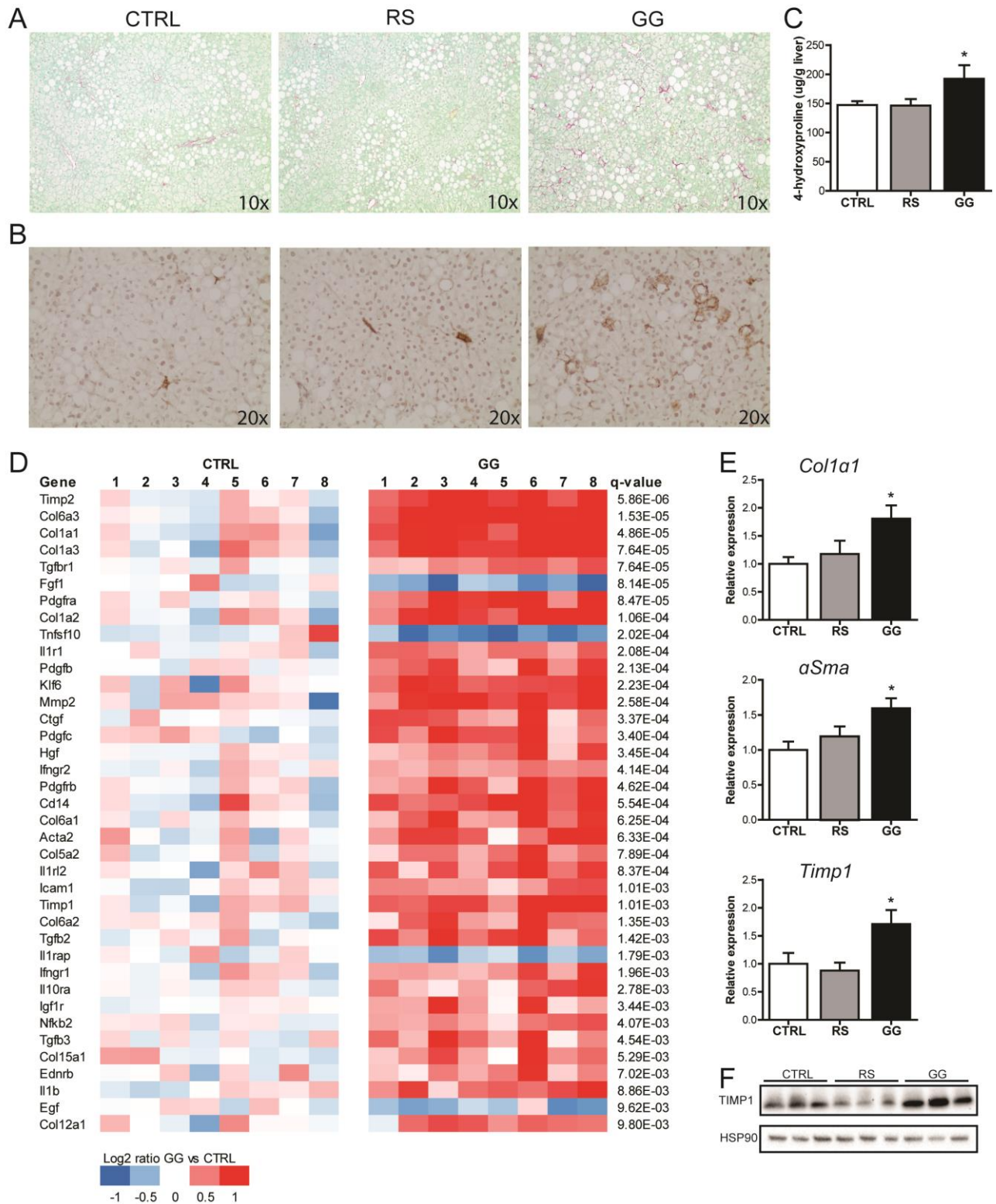


Figure 5. Stimulation of the gut microbiota by guar gum is associated with enhanced hepatic fibrogenesis

Representative pictures of liver sections stained for (A) collagen using fast green FCF/Sirius Red F3B and (B) hepatic stellate cell activation using an antibody against alpha smooth muscle actin (α SMA). (C) 4-hydroxyproline content in the liver. (D) Heat map showing significant changes in expression of genes involved in hepatic fibrosis / hepatic stellate cell activation in the livers of CTRL and GG mice. The Log₂ expression signals of the CTRL group were arbitrarily set at 0. (E) Relative expression of fibrosis-related genes in the liver. Gene expression levels in CTRL mice were set at 1. Data are presented as mean \pm SEM. Asterisks represent significant differences compared with CTRL. * p <0.05. (F) TIMP1 protein expression measured by western blotting. HSP90 was used as loading control.

Figure 6

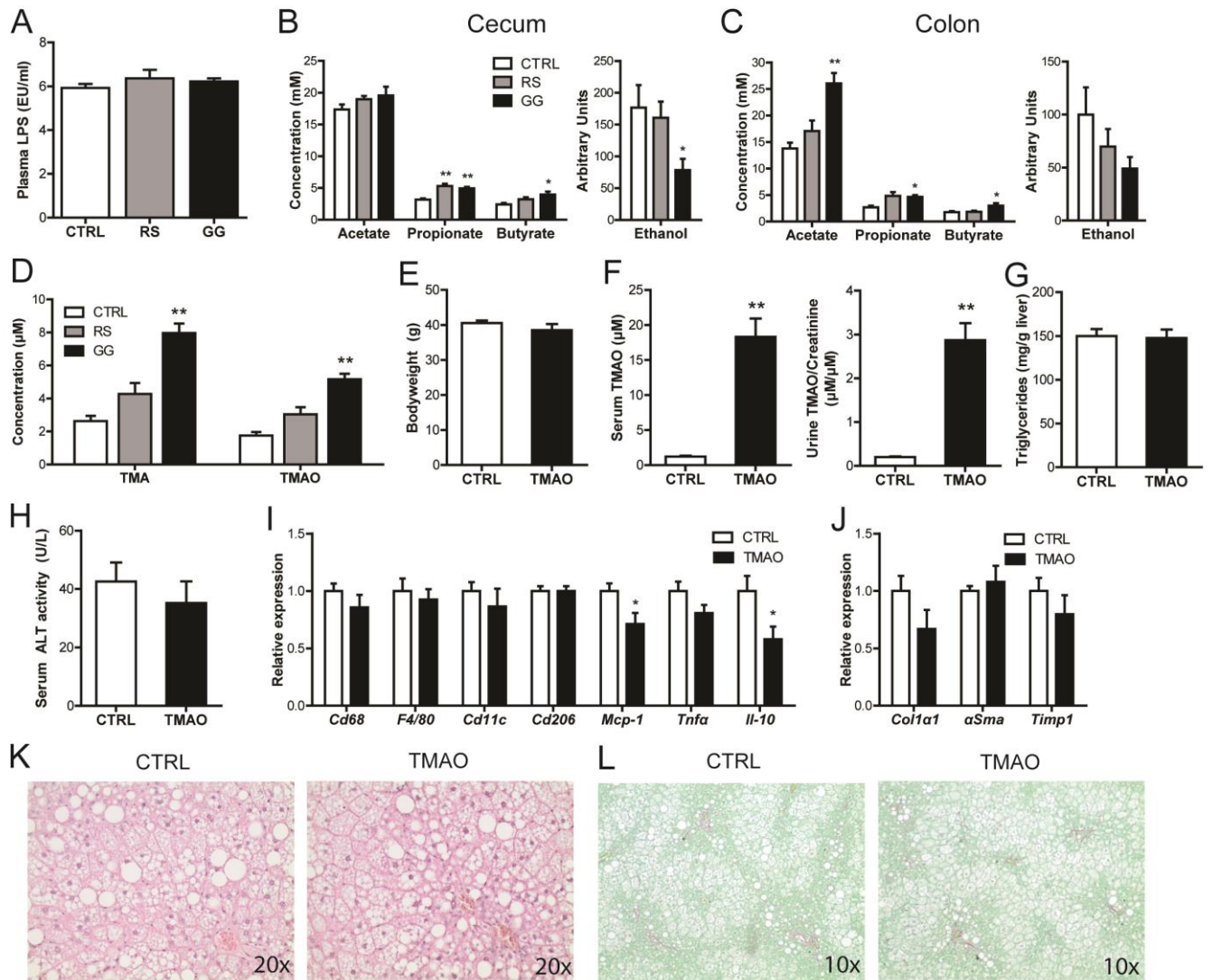


Figure 6. Guar gum-induced elevation of TMAO does not contribute to enhanced NALFD development

(A) Plasma LPS levels. (B) Cecal and (C) colonic SCFA concentration and ethanol abundance. (D) Plasma TMA and TMAO levels. (E) Final bodyweight of mice fed CTRL or TMAO-enriched diet for 18 weeks. (F) Serum and urinary TMAO levels. Urinary TMAO levels are corrected for creatinine levels to adjust for urinary dilution (G) Quantitative analysis of liver triglyceride levels. (H) Activity of alanine aminotransferase (ALT) in serum. Relative expression of (I) inflammatory and (J) fibrosis-related genes in the liver. Gene expression levels in CTRL mice were set at 1. Data are presented as mean \pm SEM. Asterisks represent significant differences compared with CTRL. * $p < 0.05$, ** $p < 0.001$. (K) H&E staining of representative liver sections. (L) Representative pictures of liver sections stained

for collagen using fast green FCF/Sirius Red F3B.

Figure 7

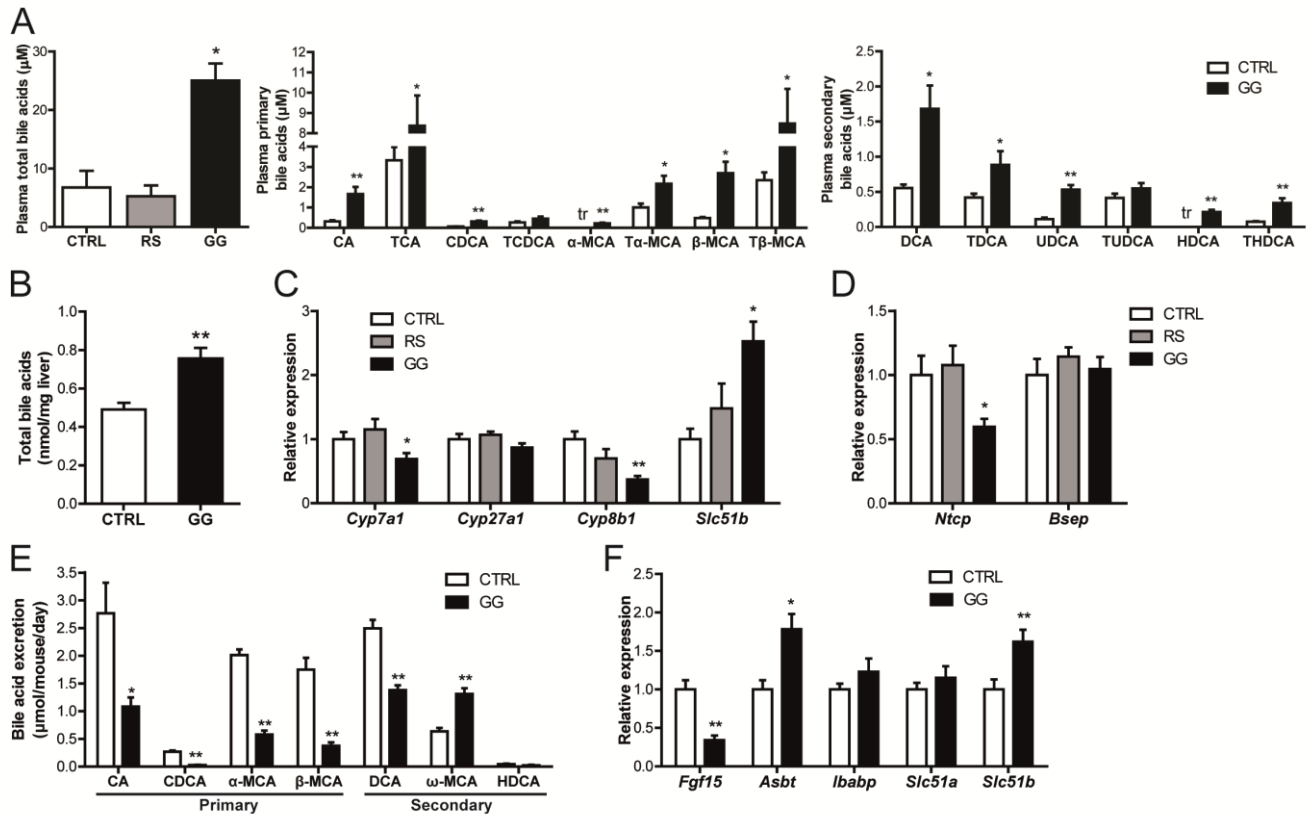


Figure 7. Guar gum elevates plasma bile acid levels likely by promoting bile acid reabsorption

(A) Total bile acid concentration in plasma of CTRL, RS and GG mice and concentration of free and conjugated primary and secondary bile acid subspecies in the plasma of CTRL and GG mice. (B) Total bile acid content in the liver of CTRL and GG mice. (C) Relative expression of genes encoding enzymes of bile acid synthesis and the FXR target gene *Slc51b* in the liver. Gene expression levels in CTRL mice were set at 1. (D) Relative expression of hepatic bile acid transporters. (E) Mean excretion of free and conjugated bile acid subspecies per mouse per day in the CTRL and GG group at the end of the dietary intervention. (F) Relative expression of *Fgf15* and bile acid transporters in the ileum. Gene expression levels in CTRL mice were set at 1. Data are presented as mean ± SEM. Asterisks represent significant differences compared with CTRL. * $p < 0.05$, ** $p < 0.001$.

Figure 8

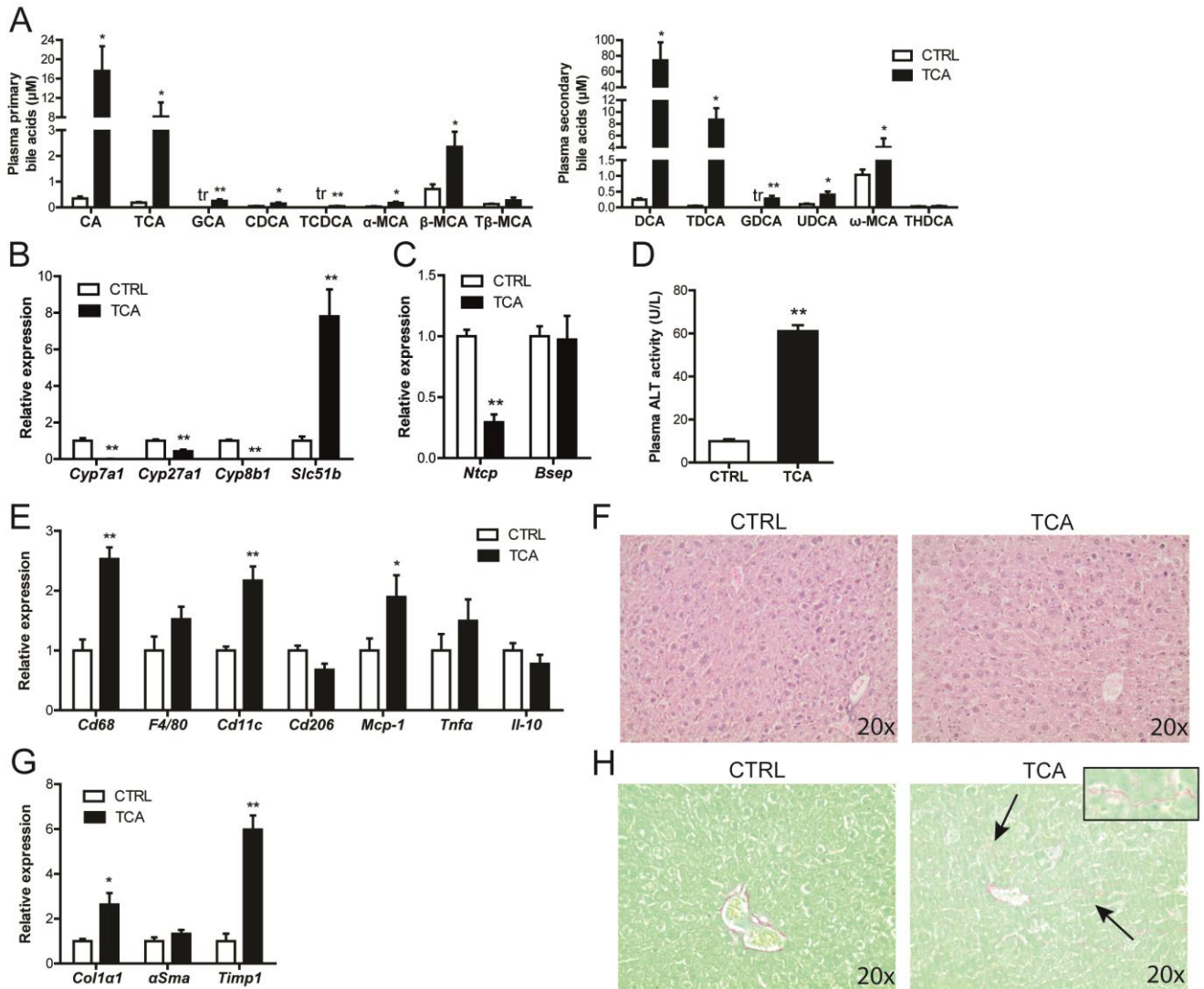


Figure 8. Bile acids promote hepatic injury

(A) Concentration of free and conjugated bile acid subspecies in the plasma of CTRL and taurocholic acid-fed mice. Tr indicates that only trace levels of this bile acid could be measured. (B) Relative expression of genes encoding enzymes of bile acid synthesis and the FXR target gene *Slc51b*. Gene expression levels in CTRL mice were set at 1. (C) Relative expression of hepatic bile acid transporters. Gene expression levels in CTRL mice were set at 1. (D) Activity of alanine aminotransferase (ALT) in plasma. (E) Relative expression of inflammatory genes in the liver. Gene expression levels in CTRL mice were set at 1. (F) H&E staining of representative liver sections. (G) Relative expression of fibrosis-related genes in the liver. Gene expression levels in CTRL mice were set at 1. (H) Representative pictures of liver sections stained for collagen using fast green FCF/Sirius

Red F3B. Inset is a higher magnification of the collagen deposition as observed in the livers of the taurocholic acid-fed mice. Data are presented as mean \pm SEM. Asterisks represent significant differences compared with CTRL. * $p < 0.05$, ** $p \leq 0.001$.

Figure 9

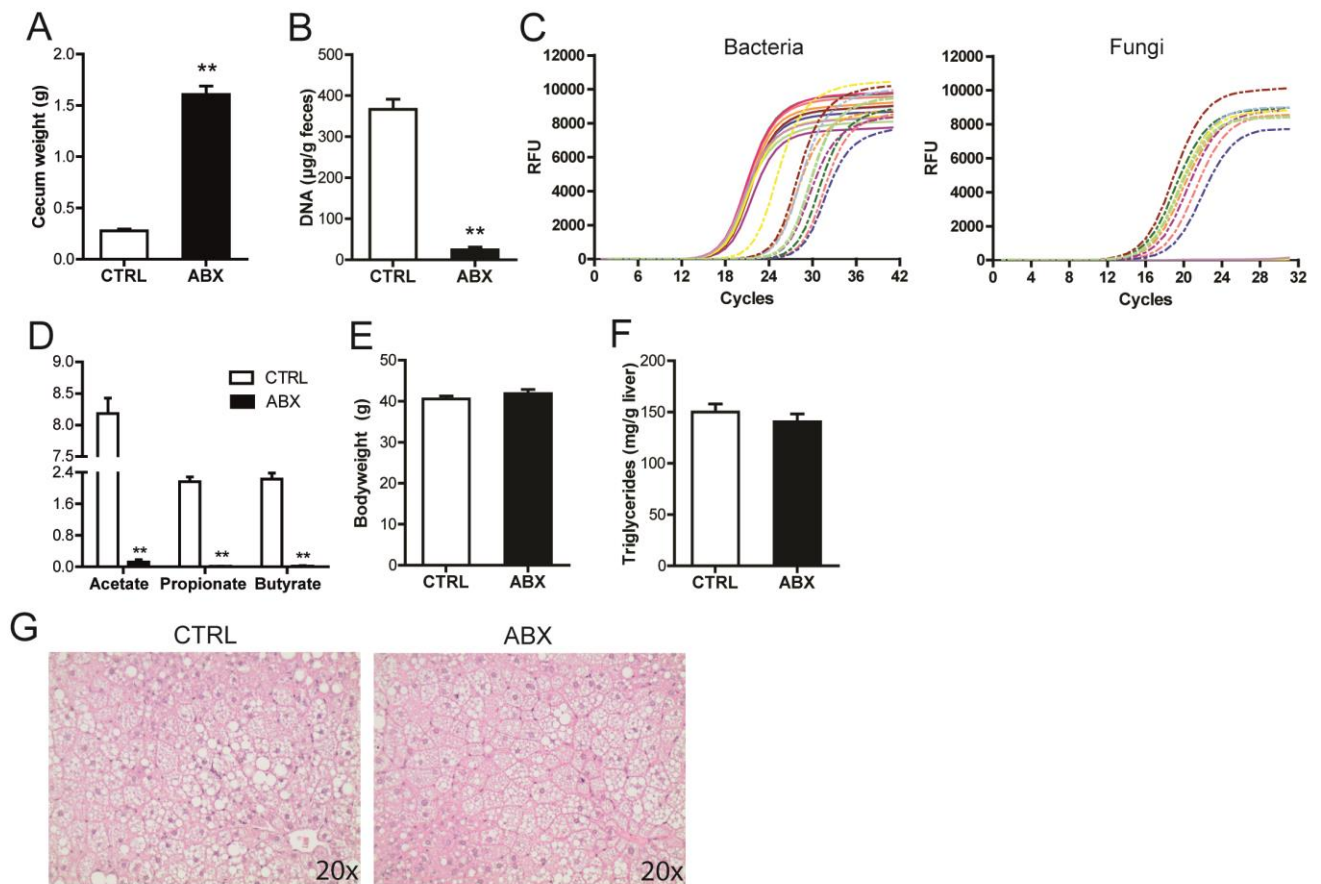


Figure 9. Suppression of the gut bacteria using antibiotics does not affect hepatic steatosis

(A) Weight of the cecum. (B) Quantitative analysis of fecal DNA levels. (C) qPCR amplification plot for 16s rRNA gene and fungal ITS1-5.8S-ITS2 region in equal amounts of fecal DNA. Solid lines indicate CTRL mice and dashed lines indicate ABX mice. (D) Cecal SCFA concentration. (E) Final bodyweight of mice fed CTRL diet with or without antibiotics supplementation. (F) Quantitative analysis of liver triglyceride levels. (G) H&E staining of representative liver sections. Data are presented as mean \pm SEM. Asterisks represent significant differences compared with CTRL. ** $p \leq 0.001$.

Figure 10

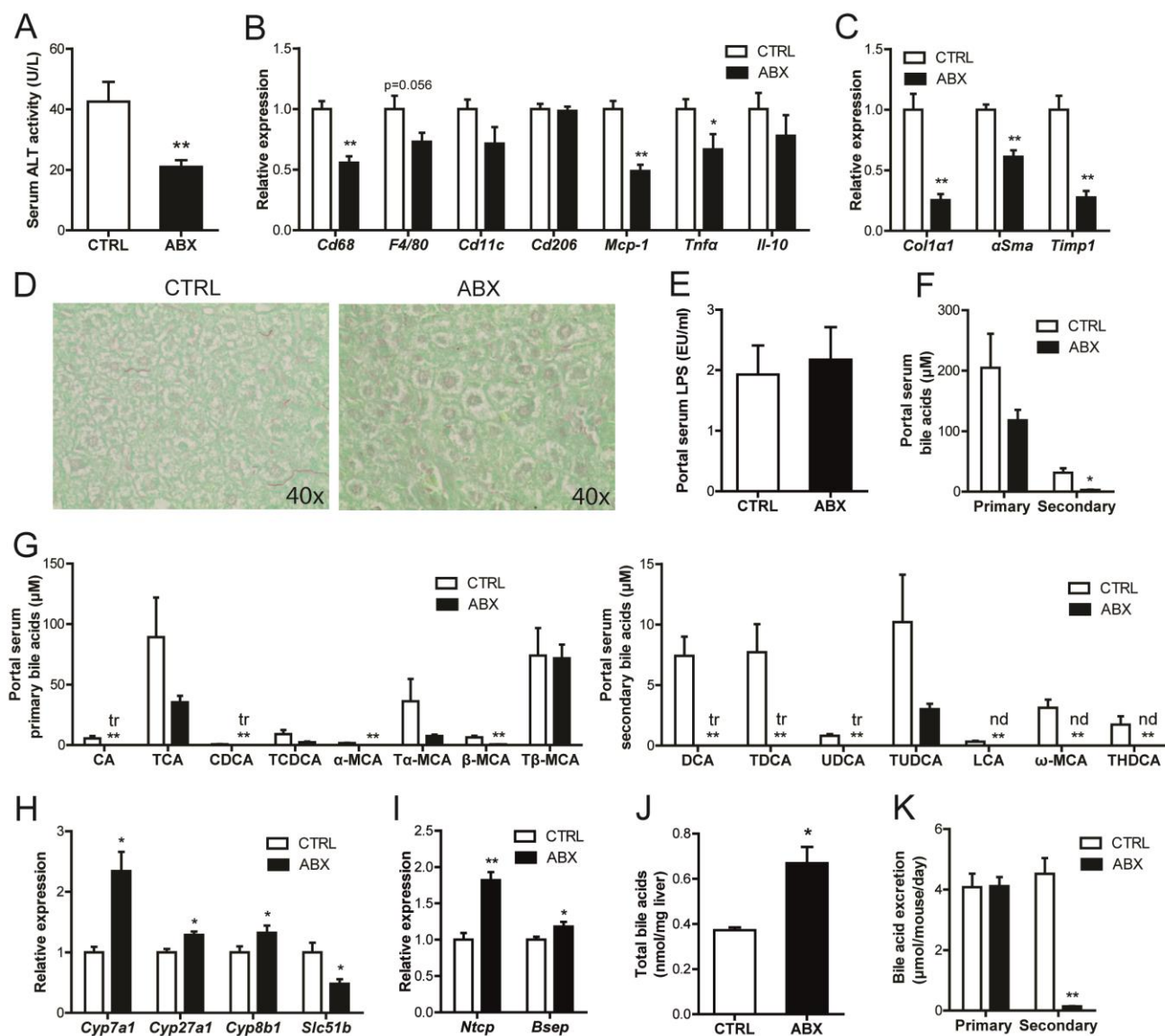


Figure 10. Antibiotics attenuate hepatic inflammation and fibrosis

(A) Activity of alanine aminotransferase (ALT) in serum. Relative expression of (B) inflammatory and (C) fibrosis-related genes in the liver. Gene expression levels in CTRL mice were set at 1. (D) Representative pictures of liver sections stained for collagen using fast green FCF/Sirius Red F3B. (E) Portal serum lipopolysaccharide levels. (F) Concentration of primary and secondary bile acids in portal serum. (G) Concentration of free and conjugated primary and secondary bile acid subspecies in the portal serum of CTRL and GG mice. Tr indicates that only trace levels of this bile acid could be measured. Nd indicates that levels of this bile acid were below detectable limit. (H) Relative expression of genes encoding enzymes of bile acid synthesis and the FXR target gene *Slc51b*. Gene

expression levels in CTRL mice were set at 1. **(I)** Relative expression of hepatic bile acid transporters. Gene expression levels in CTRL mice were set at 1. **(J)** Total bile acid content in the liver. **(K)** Mean excretion of primary and secondary bile acids per mouse per day in the CTRL and ABX group at the end of the dietary intervention. Data are presented as mean \pm SEM. Asterisks represent significant differences compared with CTRL. * $p < 0.05$, ** $p \leq 0.001$.